The V-ATPase membrane domain is a sensor of granular pH that controls the exocytotic machinery

Sandrine Poëa-Guyon,[1] Mohamed Raafet Ammar,[2] Marie Erard,[3] Muriel Amar,[1] Alexandre W. Moreau, Philippe Fossier,[1] Vincent Gleize,[1] Nicolas Vitale,[2] and Nicolas Morel[1]

[1]Centre de Neurosciences Paris-Sud, Centre National de la Recherche Scientifique Unité Mixte de Recherche 8195 and Université Paris-Sud, F-91405 Orsay, France
[2]Institut des Neurosciences Cellulaires et Intégratives, Centre National de la Recherche Scientifique Unité Propre de Recherche 3212 and Université de Strasbourg, 67084 Strasbourg, France
[3]Laboratoire de Chimie Physique, Centre National de la Recherche Scientifique Unité Mixte de Recherche 8000 and Université Paris-Sud, F-91405 Orsay, France

Several studies have suggested that the V0 domain of the vacuolar-type H^+-adenosine triphosphatase (V-ATPase) is directly implicated in secretory vesicle exocytosis through a role in membrane fusion. We report in this paper that there was a rapid decrease in neurotransmitter release after acute photoinactivation of the V0 a1-I subunit in neuronal pairs. Likewise, inactivation of the V0 a1-I subunit in chromaffin cells resulted in a decreased frequency and prolonged kinetics of amperometric spikes induced by depolarization, with shortening of the fusion pore open time. Dissipation of the granular pH gradient was associated with an inhibition of exocytosis and correlated with the V1–V0 association status in secretory granules. We thus conclude that V0 serves as a sensor of intragranular pH that controls exocytosis and synaptic transmission via the reversible dissociation of V1 at acidic pH. Hence, the V-ATPase membrane domain would allow the exocytotic machinery to discriminate fully loaded and acidified vesicles from vesicles undergoing neurotransmitter reloading.

Introduction

Vacuolar-type H^+-ATPases (V-ATPases) transport protons across the membrane of various organelles (e.g., lysosomes, endosomes, trans-Golgi network, and secretory granules), and the acidification of these organelles is required for many cellular processes (e.g., maturation or degradation of proteins, receptor-mediated endocytosis, and proton-coupled transport of small molecules; Forgac, 2007). V-ATPases are large multimeric enzymes organized in two domains, V1 and V0. The cytosolic V1 domain contains eight different subunits (A–H), with subunit A catalyzing ATP hydrolysis (Forgac, 2007). The V0 membrane domain translocates protons and contains five copies of proteolipid subunit c and single copies of subunits a, c′′, d, and e (Forgac, 2007). In vertebrates, four isoforms of subunit a (a1–a4) have been identified with specific cellular and tissues distributions (Toei et al., 2010). Four variants of a1 are generated by alternative splicing, with a1-I being specifically addressed to nerve terminals (Morel et al., 2003; Poëa-Guyon et al., 2006). The V-ATPase activity generates a large electrochemical proton gradient in synaptic vesicles in neurons and in chromaffin granules in neuroendocrine chromaffin cells, their internal pH reaching pH 5.2–5.5 (Michaelson and Angel, 1980; Füldner and Stadler, 1982) and 5.5 (Johnson and Scarpa, 1976; Pollard et al., 1979), respectively. This electrochemical proton gradient energizes the accumulation of neurotransmitters in synaptic vesicles by specific vesicular transporters or of catecholamines in chromaffin granules. A low intragranular pH is also required for catecholamine binding to chromogranins within the secretory granules (Camacho et al., 2006).

Independently of its well-established role in proton translocation, V0 has been implicated in neurotransmitter release (Hiesinger et al., 2005), in intracellular membrane fusion events

N. Vitale and N. Morel contributed equally to this paper.

Correspondence to Nicolas Morel: nicolas.morel@u-psud.fr; or Nicolas Vitale: vitalen@inci-cnrs.unistra.fr

A.W. Moreau's present address is UCL Institute of Neurology, Queen Square, London WC1N 3BG, England, UK.

V. Gleize's present address is Centre de Recherche Institut du Cerveau et de la Moëlle, Université Pierre et Marie Curie and Institut National de la Santé et de la Recherche Médicale Unité Mixte de Recherche S975, F-75651 Paris, Cedex 13, France.

Abbreviations used in this paper: AM, acetoxymethyl; CALI, chromophore-assisted light inactivation; DSP, dithiobis-succinimidyl propionate; EAP, embryonic alkaline phosphatase; FLIM, fluorescence lifetime imaging; V-ATPase, vacuolar-type H^+-ATPase.

The Rockefeller University Press $30.00
J. Cell Biol. Vol. 203 No. 2 283–298
www.jcb.org/cgi/doi/10.1083/jcb.201303104

(Peters et al., 2001; Peri and Nüsslein-Volhard, 2008; Williamson et al., 2010; Strasser et al., 2011), and in exocytosis (Liégeois et al., 2006), suggesting that V0 could be directly involved in the fusion between two membrane compartments. The exocytotic release of transmitter molecules packaged in synaptic vesicles or secretory granules is a highly regulated process that allows vesicles to fuse with the plasma membrane. This rapid process requires the formation of a fusion pore that opens and then expands, leading to full membrane fusion upon an increase in the cytosolic calcium level (Jahn and Fasshauer, 2012). Among the proteins involved in membrane fusion, the SNAREs have been proposed to constitute the core of the fusion machinery (Rizo and Rosenmund, 2008; Wickner and Schekman, 2008). The formation of a SNARE complex between the vesicle-associated SNARE VAMP-2 (synaptobrevin-2) and the plasma membrane t-SNAREs syntaxin-1 and SNAP-25 allows vesicle docking to the plasma membrane and provides the energy required for membrane fusion (Jahn and Fasshauer, 2012). It has been proposed that V0 could be a component of the fusion pore (Morel et al., 2001; Peters et al., 2001) or, alternatively, that it could favor lipid mixing and the formation of a lipidic fusion pore (El Far and Seagar, 2011; Strasser et al., 2011). Indeed, V0 has been shown to interact with SNARE proteins (Galli et al., 1996; Peters et al., 2001; Morel et al., 2003; Hiesinger et al., 2005; Di Giovanni et al., 2010). In addition, V0 could also behave as a pH sensor (Hurtado-Lorenzo et al., 2006; Hosokawa et al., 2013), which could participate in the priming steps that render secretory vesicles competent for exocytosis (Morel, 2003). These pioneer studies relied on the genetic impairment of specific V0 subunits that perturbed organelle membrane fusion while preserving their acidification. But, with long-term V0 inactivation, it is difficult to exclude the possibility that the observed membrane fusion deficits result indirectly from alterations in membrane protein or lipid metabolism or trafficking rather than from the impairment of V0 itself. The acute and selective inactivation of V0 should bypass such limitations. We thus made use of the chromophore-assisted light inactivation (CALI) technique (Tour et al., 2003; Jacobson et al., 2008). The protein of interest is genetically modified by insertion of a small TC (tetracysteine) motif, which specifically binds membrane-permeant biarsenical dyes. Upon illumination, these dyes release short-lived reactive oxygen singlets that locally and specifically inactivate the TC-tagged protein (Tour et al., 2003; Yan et al., 2006). This approach has already been successfully validated for the study of synaptic transmission in *Drosophila melanogaster* (Marek and Davis, 2002).

Our results show that the photoinactivation of the V0 a1-I subunit leads to a rapid impairment of synaptic transmission in neurons and of catecholamine release in chromaffin cells. This effect is clearly different from the delayed effect of either pharmacological inhibition of proton transport or photoinactivation of the V1 catalytic subunit A, strongly arguing that V0 regulates fusion independently from proton transport. We also observed that granule exocytosis in neurosecretory PC12 cells is dependent on the intragranular pH and that V0 appears to behave as an intragranular pH sensor that regulates the exocytotic machinery.

Results

Photoinactivation of the V0 subunit a1-I impairs neurotransmitter release

To test the effect of an acute inactivation of V0 on synaptic transmission, we expressed a TC-tagged subunit a1-I in neurons. We chose to modify this isoform of the V0 subunit a because it is present in synaptic vesicles and chromaffin granules (Morel et al., 2003; Poëa-Guyon et al., 2006; Saw et al., 2011). Synaptic transmission was then monitored in connected neuronal pairs before and immediately after the photoinactivating flash. The recombinant V0 subunit a1-I (or V1 subunit A) carrying the TC motif FLNCCPGCCMEP was generated by insertion of the motif between either an N- or C-terminal Flag tag and the a1 coding sequence (Fig. 1 A). Binding of FlAsH-EDT_2, a biarsenical derivative of fluorescein, to the TC motif allows the acute photoinactivation of the tagged protein when a brief light pulse is delivered (Tour et al., 2003). The insertion of small tags either in N- or C-terminal positions did not modify targeting of the a1-I subunit to nerve endings (Poëa-Guyon et al., 2006) or to secretory granules in PC12 or chromaffin cells (Figs. S1 and S4 C). In addition, in our experimental conditions, FlAsH-EDT_2 selectively bound to granules in PC12 cells expressing the Flag-TC–tagged a1-I subunit (Fig. S1 C). Likewise, the subcellular distribution of the V1 subunit A (Fig. S1 E) is not modified by the insertion of a Flag-TC tag at the N-terminal position (Fig. S1 D). These data illustrate that the localization of these recombinant V-ATPase subunits matched that of the endogenous proteins.

Neurons in primary culture were transfected to coexpress GFP and the recombinant V-ATPase subunit. The release of neurotransmitter from GFP-expressing neurons was monitored by recording postsynaptic currents elicited by a series of single action potentials delivered at 0.03 Hz to the presynaptic element in neuronal pairs (Figs. 1, B and C; and S2), before and after a 1-min photoinactivating flash. The photoinactivation procedure did not affect the baseline neurotransmitter release from neurons that express GFP alone (Fig. 1 C, open circles). In contrast, neurotransmitter release from neurons expressing the TC-tagged a1-I was dramatically decreased after the flash (Fig. 1 C, filled circles). This decrease occurred within 2 min after the flash, and the postsynaptic response amplitude then stabilized to a plateau that was maintained for several minutes. This was observed with both GABAergic and glutamatergic neurons expressing the recombinant a1-I, and the position of the TC tag (N vs. C terminal) did not affect the outcome of photoinactivation (Figs. 1 C and S2 A). When averaged across the whole dataset, the decrease in the postsynaptic response amplitude was 50.3 ± 6.0% ($P < 0.001$, $n = 6$; Fig. 1 D). The observed effect appeared to be independent of the transport of protons by the V-ATPase because incubation of neurons with the specific V-ATPase inhibitor concanamycin A did not impair the baseline neurotransmitter release (spikes frequency of 0.03 Hz) monitored for over 10 min (Fig. S2 B). However, increasing spike frequency to 1 Hz in the presence of concanamycin A led to a rapid and important suppression of synaptic transmission (Fig. S2 B) as previously reported (Hong, 2001; Cavelier and

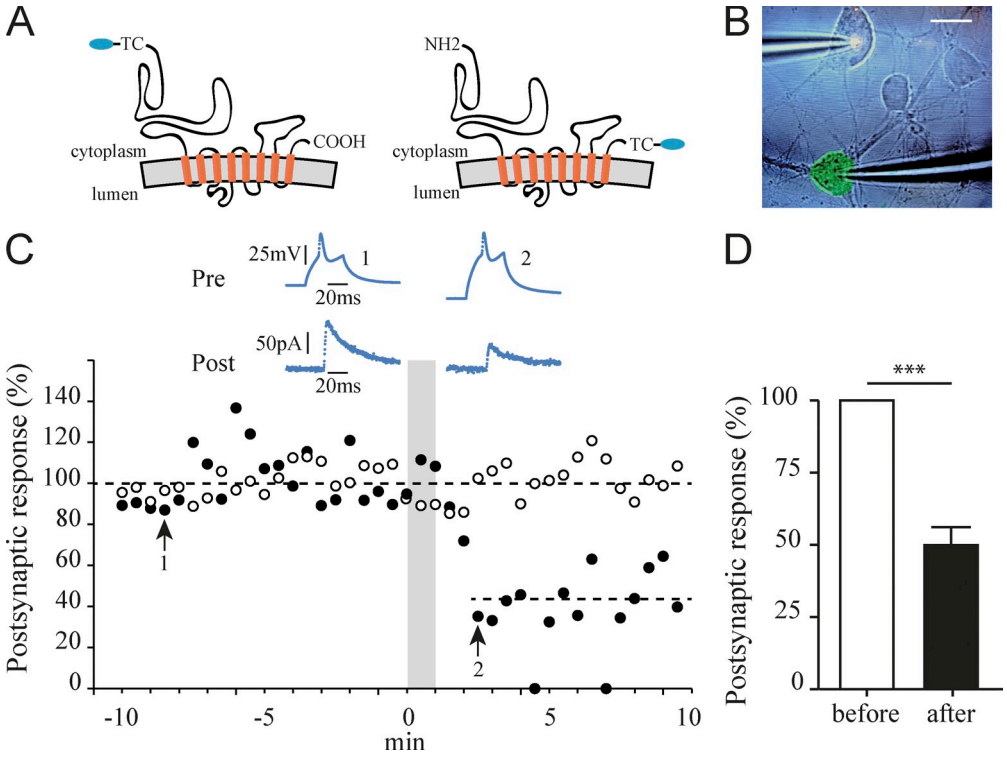

Figure 1. **Photoinactivation of the a1-I subunit of V0 impairs synaptic transmission.** (A) Representation of the V0 a1-I subunit with the Flag (blue) and TC tags in the N- or C-terminal position. (B) Micrograph illustrating the experimental configuration with a patch-clamped presynaptic GFP-expressing neuron (stimulated neuron, colorized in green) and a connected untransfected neuron (voltage clamped to measure the postsynaptic response). Bar, 20 µm. (C) Evolution of the postsynaptic current amplitude in response to presynaptic action potentials (stimulation every 30 s) of rat hippocampal neurons expressing GFP alone (open circles) or GFP + V0 TC-tagged a1-I subunit (filled circles). Current amplitudes were expressed in the percentage of their mean amplitude before the photoinactivating flash. Neurons were successively incubated with 1 µM FlAsH-EDT_2 for 10 min and 1 mM BAL without modification of the postsynaptic responses. Photoinactivation was carried for 1 min (gray area). Data shown are from single representative experiments out of three (open circles) or four (filled circles). Typical presynaptic action potentials (Pre) and postsynaptic responses (Post) either before (1) or after (2) the flash are shown. Dotted lines correspond to the mean amplitude of the postsynaptic responses before (top line) or after the photoinactivating flash (bottom line). (D) Averaged effects of V0 a1-I subunit photoinactivation on synaptic transmission. Pooled results include six neuronal pairs, either GABAergic or glutamatergic (paired Student's *t* test).

Attwell, 2007). In addition, neurotransmitter release from neurons expressing a V1 subunit A with an N-terminal TC tag was not photoinactivated (unpublished data). These data show that the photoinactivation of the V0 a1-I subunit of nerve endings results in a rapid (within 2 min) and large (50%) decrease in the release of transmitter, which is independent of the transport of protons by the V-ATPase.

Photoinactivation of the V0 a1-I or the V1 A subunits have different effects on the release of catecholamines

To investigate the mechanisms underlying the decrease in neurotransmission, we conducted similar photoinactivation experiments on chromaffin cells expressing Flag-TC–tagged V-ATPase subunits. Here, we monitored the exocytosis of catecholamines (triggered by KCl depolarization) by carbon fiber amperometry (Vitale et al., 2001; Chasserot-Golaz et al., 2005) and gained direct access to several exocytosis parameters (Fig. 2 C). Catecholamine release from untransfected or GFP-expressing cells was not affected by incubation with FlAsH-EDT_2 and BAL (2,3-dimercapto-1-propanol) or by illumination (Table S1). Furthermore, catecholamine release from chromaffin cells expressing recombinant V-ATPase subunits, either the V0 a1-I subunit with N- or C-terminal tags or the V1 A subunit with an N-terminal Flag-TC tag, was identical to that of untransfected cells (Table S1). This showed that the insertion of the TC and Flag tags in these V-ATPase subunits did not impair the enzyme activity, granule acidification, and catecholamine content. We estimated the relative amounts of the endogenous and recombinant V0 a1 subunits in transfected PC12 cells that coexpress the Flag-TC–tagged a1-I subunit and GFP. The total a1 subunit content in cells increased by 132 ± 6% ($n = 3$) after transfection, whereas the subunit c content was not affected (Fig. S3). Considering that only 7% of cells were effectively transfected in these conditions, we can estimate that the level of recombinant a1 subunit is four to five times higher than that of endogenous a1 in transfected cells.

Illumination of chromaffin cells transfected with the TC-tagged a1-I subunit (either in N- or in C-terminal position) modified catecholamine release as shown by the decrease in the exocytotic spike frequency (Fig. 2, A and B, 5 min after flash). Although the total amount of current during the spikes was not modified, the half width was increased, and the mean spike amplitude was reduced (Fig. 2 D). In agreement with the notion that spikes were smaller and broader, we also found a significant increase in the rise time value in cells expressing

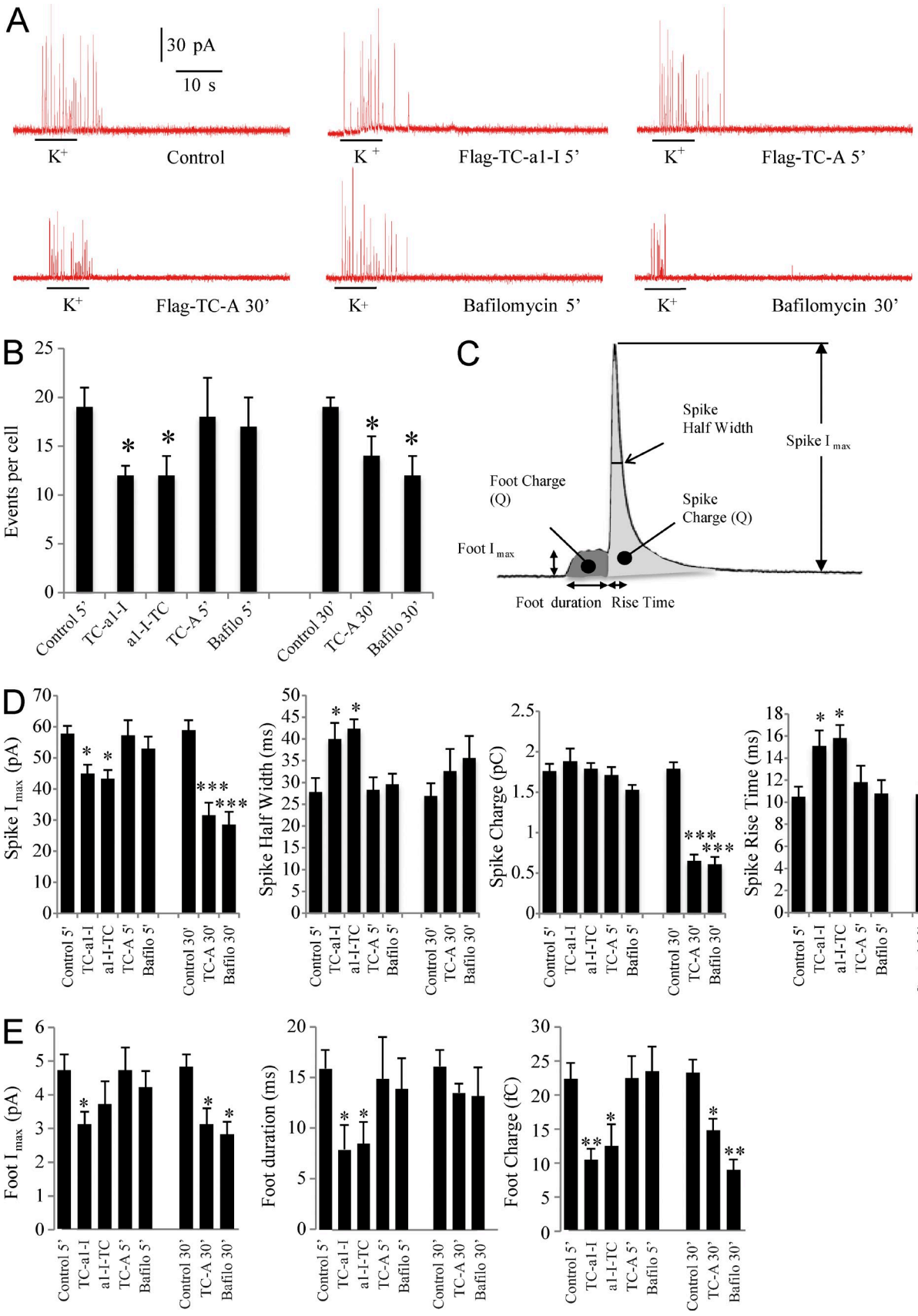

Figure 2. **Photoinactivation of the V0 a1-I or V1 A subunits impairs chromaffin cell catecholamine release in different ways.** Chromaffin cells coexpressing either the V0 a1-I or the V1 A subunits bearing a Flag-TC tag and GFP were successively incubated with the FlAsH-EDT$_2$ probe that specifically binds to the TC motif and 1 mM BAL. Photoinactivation was obtained by a 1-min illumination. Catecholamine release was evoked by a 10-s application of 100 mM

TC-tagged V0 a1-I and illuminated (Fig. 2 D). Furthermore, significant variations in the prespike or foot parameters were observed (Fig. 2 E). Although the percentage of the spikes that presented a detectable foot was not modified (~25% in the different conditions), chromaffin cells exhibited significantly shorter feet (nearly twofold reduction in duration) after photoinactivation of V0 a1-I, with a significant reduction in amplitude. Consequently, the total foot charge was dramatically reduced after V0 a1-I photoinactivation. Altogether, these results showed that V0 a1-I photoinactivation modifies the fusion pore characteristics as well as the frequency and kinetics of exocytotic events without altering the granule catecholamine content.

Photoinactivation of the catalytic V1 subunit A yielded dramatically different results. Indeed, no significant changes in the release frequency nor in the spike or foot parameters were observed when cells were recorded shortly (5 min) after the flash (Fig. 2, A and D). However, when cells were recorded 30 min after the flash, a nearly twofold decrease in the peak current amplitude and in the total amount of current in the spikes was observed, with no significant changes in the spike frequency or kinetics (Fig. 2, A and D). The mean current of the recorded feet was significantly decreased, whereas their duration remained unchanged (Fig. 2 E). These effects most probably reflect an inhibition of proton transport by chromaffin granule V-ATPases because they were very similar to those observed after application of bafilomycin A1, a specific V-ATPase inhibitor (Fig. 2, A and D). Thus, the decrease in current amplitude observed after a 30-min V-ATPase inhibition most likely reflects a decrease in the catecholamine content of granules with no change in the exocytosis itself.

Using siRNAs targeting bovine a1 mRNAs, we reduced the amount of endogenous a1 subunit expressed after 96 h by 60% (Fig. S4, A and B). This reduction was associated with modifications of catecholamine release measured by amperometry (Fig. S4 D). All parameters of the amperometric response measured were affected, showing that both the granule catecholamine content and exocytosis were affected. All these defects were effectively rescued by coexpressing the rat a1-I subunit resistant to the siRNAs targeting the bovine sequence (Fig. S4 D), suggesting that this recombinant subunit is correctly incorporated in a functional granule V-ATPase.

In summary, photoinactivation of two subunits of the same protein complex resulted in very different alterations in catecholamine release, with inactivation of the V0 a1-I subunit affecting the fusion pore stability and exocytosis, whereas inactivation of the catalytic V1 A subunit impaired progressively the catecholamine content of secretory granules. This illustrates the exquisite selectivity of the CALI procedure. In addition, the rapidity and temporal control of V0 inactivation allowed by the CALI procedure rendered possible the description of a V0-specific effect on exocytosis occurring before the appearance of the V1–V0-dependent effects on the granular catecholamine content, and this had not been possible after silencing of the endogenous V0 a1 expression.

Granule exocytosis is inhibited after dissipation of the intragranular pH gradient

Even though V-ATPase–dependent proton transport is not required for transmitter release, the intragranular pH might still be a critical parameter for granule exocytosis. To test this hypothesis, we used neurosecretory PC12 cells and measured in parallel the pH of their secretory granules and exocytosis after various pharmacological treatments expected to affect the intragranular pH.

Measurements of catecholamine release cannot be used to follow exocytosis because catecholamines leak out into the cytosol when the granular pH raises (Camacho et al., 2006). Therefore, we generated a PC12 cell line (2B2) that stably expresses a protein of the granule matrix, CgA (chromogranin A), fused with embryonic alkaline phosphatase (EAP), allowing a sensitive measure of granule exocytosis (Taupenot et al., 2005). This chimeric protein was correctly targeted to chromaffin granules (Fig. S1) and remained inside the secretory vesicles independently of their internal pH. A second cell line (2B2-95) that stably expresses CgA-EAP and a V0 a1-I subunit carrying an N-terminal Flag-TC tag was also generated to allow the purification of the granular V-ATPase.

We took advantage of the pH sensitivity of the fluorescence lifetime of the ECFP and developed a method that allows the measurement of the intragranular pH in living PC12 cells (Poëa-Guyon et al., 2013). 2B2 or 2B2-95 PC12 cells were transfected to express CgA-ECFP that was correctly targeted to the secretory granules (Poëa-Guyon et al., 2013). Fluorescence lifetime imaging (FLIM) of CgA-ECFP within secretory granules was performed at 37°C on cells incubated with nigericin-containing KCl solutions buffered at varying pH. The fluorescence lifetime of CgA-ECFP increased from 1.40 to 2.05 ns as the pH was raised from pH 5.0 to 7.0 (Fig. 3 A). A calibration curve was established for further conversion of the fluorescence lifetime data into intragranular pH

KCl onto the recorded cell and measured by carbon fiber amperometry. Control release was measured from untransfected cells in the same culture dish or from cells that express GFP alone (both submitted to the FlAsH-EDT$_2$ and BAL treatments and the flash of light). For comparison, catecholamine release from untransfected cells that were only treated by 0.4 µM bafilomycin A1 was measured in parallel. (A) Typical amperometric recordings from a control cell (control); a cell expressing the V0 recombinant a1-I subunit, 5 min after the photoinactivating flash (Flag-TC-a1-I 5′); cells expressing the V1 recombinant A subunit, 5 or 30 min after the flash (Flag-TC-A 5′ and 30′, respectively); and untransfected cells after 5 or 30 min of bafilomycin A1 application (bafilomycin 5′ and 30′, respectively). (B) Number of amperometric spikes detected per cell in the various conditions (means ± SD from 25 to 55 cells). Control cells, 5 or 30 min after the flash (control 5′ and 30′, respectively); cells expressing the V0 a1-I subunit with the Flag-TC tag in N- or C-terminal position, 5 min after the flash (TC-a1-I and a1-I-TC); cells expressing the V1 Flag-TC-A subunit, 5 and 30 min after the flash (TC-A 5′ and TC-A 30′, respectively); and cells bafilomycin A1 treated for 5 or 30 min (bafilo 5′ and 30′). (C) Scheme showing the different parameters of the amperometric response that were measured. A foot current was detected for ~20–30% of amperometric spikes, regardless the conditions tested. (D) Main characteristics of amperometric spikes in the different conditions tested (as in B). (E) Characteristics of foot currents in the different conditions tested (as in B). Data are means ± SEM (except for B). *, $P < 0.05$; ***, $P < 0.001$.

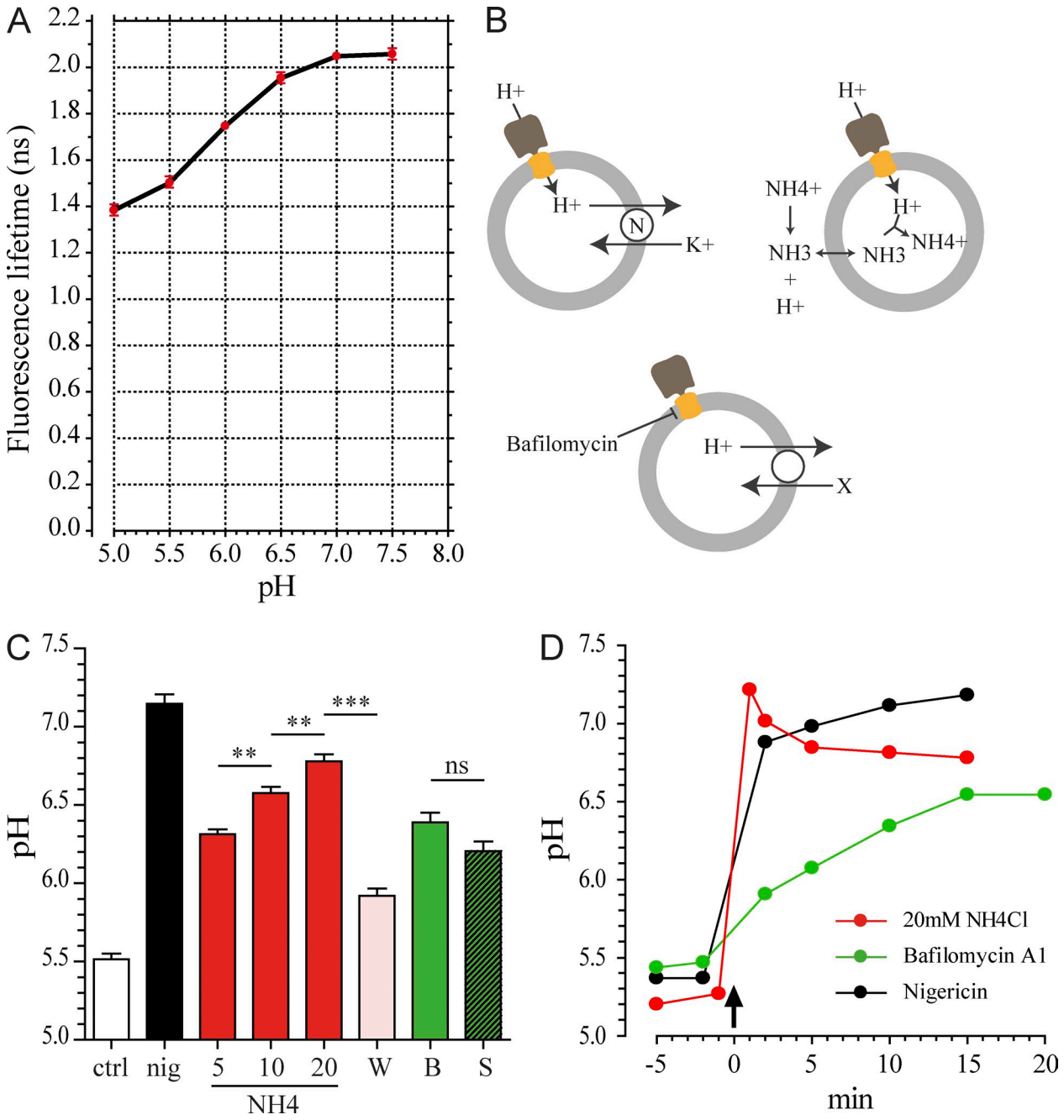

Figure 3. **Manipulation of intragranular pH in PC12 cells.** PC12 cells expressing CgA-ECFP were used to measure intragranular pH using FLIM. (A) Calibration curve of fluorescence lifetimes of CgA-ECFP in the function of intragranular pH. PC12 cells were incubated in calibration solutions that contain 10 µM nigericin and 140 mM KCl buffered at the indicated pH. Data are means ± SEM (n = 15–42 cells from six independent experiments). (B) Schemes illustrating how nigericin (N), NH_4Cl, or V-ATPase inhibitors affect intragranular pH. (C) Intragranular pH plateau values measured in various conditions. In resting conditions (control [ctrl]) pH was 5.51 ± 0.04 (n = 92 cells). After treatment with 5 µM nigericin (nig), granular pH was 7.15 ± 0.06 (n = 30). Increasing concentrations of NH_4Cl led to increasing granular pH, 6.31 ± 0.03 (n = 23) at 5 mM, 6.58 ± 0.04 (n = 37) at 10 mM, and 6.78 ± 0.04 (n = 46) at 20 mM, an effect that was reversible after washing (W) out NH_4Cl, pH 5.92 ± 0.05 (n = 20). The V-ATPase inhibitors bafilomycin A1 (B) and saliphenylhalamide A (S) at 0.4 µM raised the pH to 6.80 ± 0.05 (n = 13) and 6.21 ± 0.06 (n = 19), respectively. **, P < 0.01; ***, P < 0.001. (D) Time course of granular pH variations after NH_4Cl, bafilomycin A1, or nigericin addition (arrow). Typical experiments are shown that were repeated at least four times.

values (Fig. 3 A). Under physiological conditions, the intragranular pH was identical for 2B2 and 2B2-95 cell lines (5.51 ± 0.04, n = 92), showing that expression of a tagged a1-I subunit did not affect H^+ translocation by the V-ATPase. This value is in good agreement with previously reported determinations measured by alternative methods (Johnson and Scarpa, 1976; Pollard et al., 1979).

Then, we used nigericin, NH_4Cl, or V-ATPase inhibitors to manipulate the intragranular pH (Fig. 3 B). Nigericin is a K^+ ionophore that exchanges protons for K^+. NH_4Cl is in equilibrium with the weak base NH_3, which is membrane permeable and enters acidic compartments where it binds a proton. These two treatments lower the granular pH gradient with little effect on the granular transmembrane potential. Inhibition

of V-ATPase activity by specific inhibitors (concanamycin A, bafilomycin A1, and saliphenylhalamide A) blocks proton entry into the granules, and the proton gradient progressively dissipates through consumption of internal protons in exchange for substrates by various granular transporters (Fig. 3 B). The FLIM approach allowed repetitive pH measurements, before and after application of the drugs (Fig. 3 D), and estimations of the kinetics of the granular pH changes. From all pH modulators tested, nigericin was the most efficient and raised rapidly the intragranular pH to a plateau value of 7.15 ± 0.06 (Fig. 3, C and D). The effect of NH_4Cl on the granular pH was dose dependent and reversible, with the granular pH going from 6.78 ± 0.04 in the presence of 20 mM NH_4Cl to 5.92 ± 0.05 after the wash (Fig. 3 C). In contrast to nigericin and NH_4Cl, the effect of V-ATPase inhibitors on the granular pH developed slowly (Fig. 3 D), with the granular pH gradient clearly dissipating after 15 min (Fig. 3 C). Hence, these different treatments were used to monitor the influence of the granular pH on exocytosis.

Chromaffin granule exocytosis was estimated by measuring CgA-EAP release after depolarization of 2B2 or 2B2-95 PC12 cells. NH_4Cl treatment reduced CgA-EAP release in a dose-dependent manner (Fig. 4, A and B), an effect completely reversed after NH_4Cl washout, although the reversion was less efficient in the presence of concanamycin A, suggesting that it is partially dependent on V-ATPase activity (Fig. 4 A). Inhibition of CgA-EAP release was even stronger after nigericin treatment (>75% inhibition of release), but washing did not reverse this effect (Fig. 4 C). When nigericin-treated cells were washed in the presence of the K^+ ionophore valinomycin (allowing K^+ to escape from secretory granules), a significant recovery of CgA-EAP exocytosis was observed, an effect partially inhibited by concanamycin A (Fig. 4 C). Two V-ATPase inhibitors, bafilomycin A1 or concanamycin A, sharing the same binding site on V0 (Bowman et al., 2006) and having similar effects on V-ATPase activity, did not affect CgA-EAP release (Fig. 4 D). Saliphenylhalamide A, another V-ATPase inhibitor that binds to a different site on V0 (Xie et al., 2004), decreased CgA-EAP release by 20% (Fig. 4 D). Therefore, with the exception of bafilomycin A1 and concanamycin A, treatments that raise the intragranular pH inhibited exocytosis of CgA-EAP, an effect that was in a large part reversible (Fig. 4 E).

The effects of intragranular pH modulators are independent from Ca^{2+} influx, internal calcium stores, or ATP metabolism

Because exocytosis is triggered by the influx of calcium through voltage-dependent calcium channels that open after cell depolarization, we first tested whether the decreased exocytosis observed in the presence of nigericin or NH_4Cl could be caused by a weaker influx of external calcium. When Fura-2–loaded PC12 cells were maintained under resting conditions and in the absence of external calcium, the cytosolic Ca^{2+} concentration remained low and stable even in the presence of 20 mM NH_4Cl. Nigericin triggered a progressive increase in the basal Ca^{2+} level, probably through a release from internal stores (Fig. 5 A), but this cytosolic Ca^{2+} raise was insufficient to trigger any CgA-EAP release (not depicted). When cells were depolarized in the presence of calcium, their cytosolic Ca^{2+} levels increased rapidly and remained high as long as the KCl depolarization was maintained (Fig. 5 A). However, this Ca^{2+} influx was not affected by nigericin or NH_4Cl treatments (Fig. 5 B). In addition, NH_4Cl inhibited the exocytosis of CgA-EAP to the same extent when it was induced by the calcium ionophore A23187 in the presence of external Ca^{2+} or by KCl depolarization (Fig. 5 C). All these data strongly argue that the inhibitory effects of NH_4Cl and nigericin on exocytosis were not linked to an alteration of the influx of Ca^{2+} through voltage-dependent calcium channels.

We then tested the involvement of internal calcium stores on the exocytosis of CgA-EAP either by incubation with thapsigargin, an inhibitor of the reticular calcium pump, or by addition of the calcium ionophore A23187 in the absence of external calcium (Fig. 5 D). These treatments did not trigger any significant increase of the basal CgA-EAP release in resting conditions (unpublished data). Upon KCl depolarization, CgA-EAP exocytosis was increased after A23187 or thapsigargin treatments, as compared with control conditions (Fig. 5 D), demonstrating that the release inhibition observed after nigericin or NH_4Cl treatments could not be attributed to perturbations of intracellular calcium stores.

Finally, we excluded a possible metabolic effect via an inhibition of mitochondrial ATP synthesis because oligomycin A, a specific inhibitor of mitochondrial F1F0-ATPase, induced only a moderate inhibition of CgA-EAP release (Fig. S5 A). Valinomycin, a K^+ ionophore, had no effect on CgA-EAP exocytosis (Fig. S5 B).

Altogether, these experiments showed that nigericin and NH_4Cl treatments had an effect on CgA-EAP release, which was independent from Ca^{2+} influx, depletion of internal calcium stores, or ATP metabolism. Because the inhibition of CgA-EAP release after nigericin or NH_4Cl treatments appeared to be correlated to variations of the intragranular pH (Fig. 4 E), we propose that the intrinsic exocytotic machinery could be controlled by the intragranular pH status.

V-ATPase, a sensor of intragranular pH for the exocytotic machinery?

In marked contrast with the granular pH elevation induced by nigericin or NH_4Cl treatments, the inhibition of V-ATPase activity by bafilomycin A1 and concanamycin A induced a dissipation of the granular pH gradient that was not associated with a modification of CgA-EAP release (Fig. 4 E). To test whether binding of these V-ATPase inhibitors directly perturbs the control of exocytosis by the intragranular pH, cells were incubated with V-ATPase inhibitors before nigericin or NH_4Cl treatments. Indeed, preincubation with V-ATPase inhibitors, which did not significantly alter the effect of nigericin or NH_4Cl treatments on the intragranular pH (unpublished data), impacted their effect on CgA-EAP release. Inhibition of CgA-EAP release by 20 mM NH_4Cl (Fig. 6 A) or nigericin (Fig. 6 B) was less pronounced after a preincubation with bafilomycin A1, concanamycin A, or saliphenylhalamide A. Notably, binding of bafilomycin A1 to the V-ATPase V0 domain protected CgA-EAP release more efficiently than binding of saliphenylhalamide A, in both treatments.

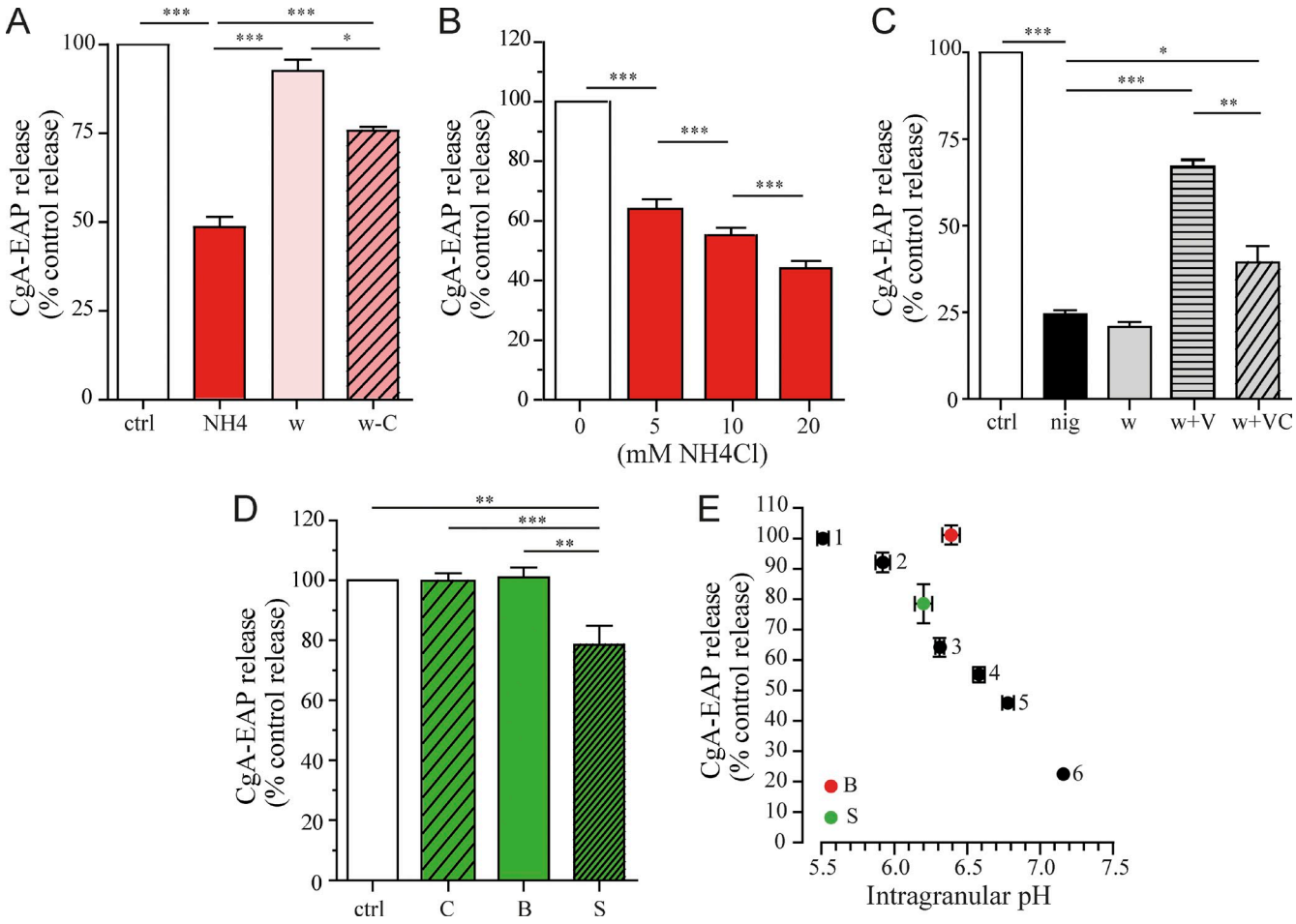

Figure 4. **Treatments that dissipate the granular pH gradient affect exocytotic release of CgA-EAP from PC12 cells.** (A) PC12 cells stably expressing CgA fused with EAP (CgA-EAP) were used to estimate exocytosis of secretory granules induced by KCl depolarization (control [ctrl]). Preincubation with 20 mM NH_4Cl for 15 min decreased CgA-EAP release by 52% (NH4), and this was reversed by NH_4Cl washout (w). Washing performed in the presence of concanamycin A (w – C) led to partial reversion. (B) Dose dependence of the effect of NH_4Cl on CgA-EAP release. Release was 64.2 ± 3.1 (n = 10), 55.2 ± 2.5 (n = 13), and 44.4 ± 2.2% (n = 19) of control release at 5, 10, and 20 mM NH_4Cl, respectively. (C) A 15-min preincubation with 5 µM nigericin (nig) markedly reduced CgA-EAP release: 24.4 ± 1.2% (n = 19) of control release. This effect was not reversed after removal of nigericin (washing), 20.8 ± 1.5% (n = 11), unless the K^+ ionophore valinomycin (5 µM) was present (washing + valinomycin [V]), a partial reversion that was inhibited by 0.4 µM concanamycin A (washing + valinomycin and concanamycin A [VC]). (D) Effects of 0.4 µM V-ATPase inhibitors. Concanamycin A (C) or bafilomycin A1 (B) did not affect CgA-EAP release, with 99.8 ± 2.5 (n = 25) and 101.1 ± 3.1% (n = 21) of control release, respectively. Saliphenylhalamide A (S) slightly but significantly depressed CgA-EAP release, with 78.5 ± 6.5% (n = 12) of control release. (E) Correlation of CgA-EAP release and intragranular pH in the presence of vehicle (1); reversion of 20 mM NH_4Cl (2); 5, 10, and 20 mM NH_4Cl (3, 4, 5, respectively); nigericin (6); bafilomycin A1 (B); and saliphenylhalamide A (S). Data are means ± SEM. *, P < 0.05; **, P < 0.01; ***, P < 0.001.

Because the V1 and V0 domains of V-ATPase can reversibly dissociate in different physiological situations (Toei et al., 2010), we tested whether the V1–V0 association was modified in conditions affecting the intragranular pH. We estimated the relative amounts of V1 associated to V0 in chromaffin granules isolated from the 2B2-95 PC12 cell line, under resting conditions or after a 15-min incubation with nigericin or bafilomycin A1 (Fig. 6 C). Cells were treated while attached to collagen-coated culture flasks. After the 15-min incubation, V1–V0 interacting domains were cross-linked by dithiobis-succinimidyl propionate (DSP; see Morel et al., 1998) to preserve their association during disruption of the cells and isolation of chromaffin granules in sucrose density gradients. Granules were followed by their CgA-EAP content. The amount of V0 was estimated by probing the endogenous V0 c subunit or the a1-I subunit carrying a Flag tag on Western blots. V1 was detected using antibodies to the catalytic A subunit. After normalization at equal V0 contents, the relative amount of A subunit associated to chromaffin granules after nigericin treatment significantly increased compared with the resting conditions (254 ± 37%, n = 3), whereas it was lower after bafilomycin A1 binding (Fig. 6 C). The amount of A associated to granules after nigericin treatment was ∼300% of that found after incubation with bafilomycin A1 (Fig. 6, F and G). When cells were pretreated with bafilomycin A1 before nigericin treatment, the amount of A associated to the granules was only increased by ∼50% (Fig. 6, D and E), indicating that bafilomycin A1 binding to V0 favored the dissociation of V1 from V0. In contrast, larger amounts of A were associated to granules after saliphenylhalamide binding (Fig. 6 E), in accordance with previous data obtained with the salicylihalamide A analogue (Xie et al., 2004).

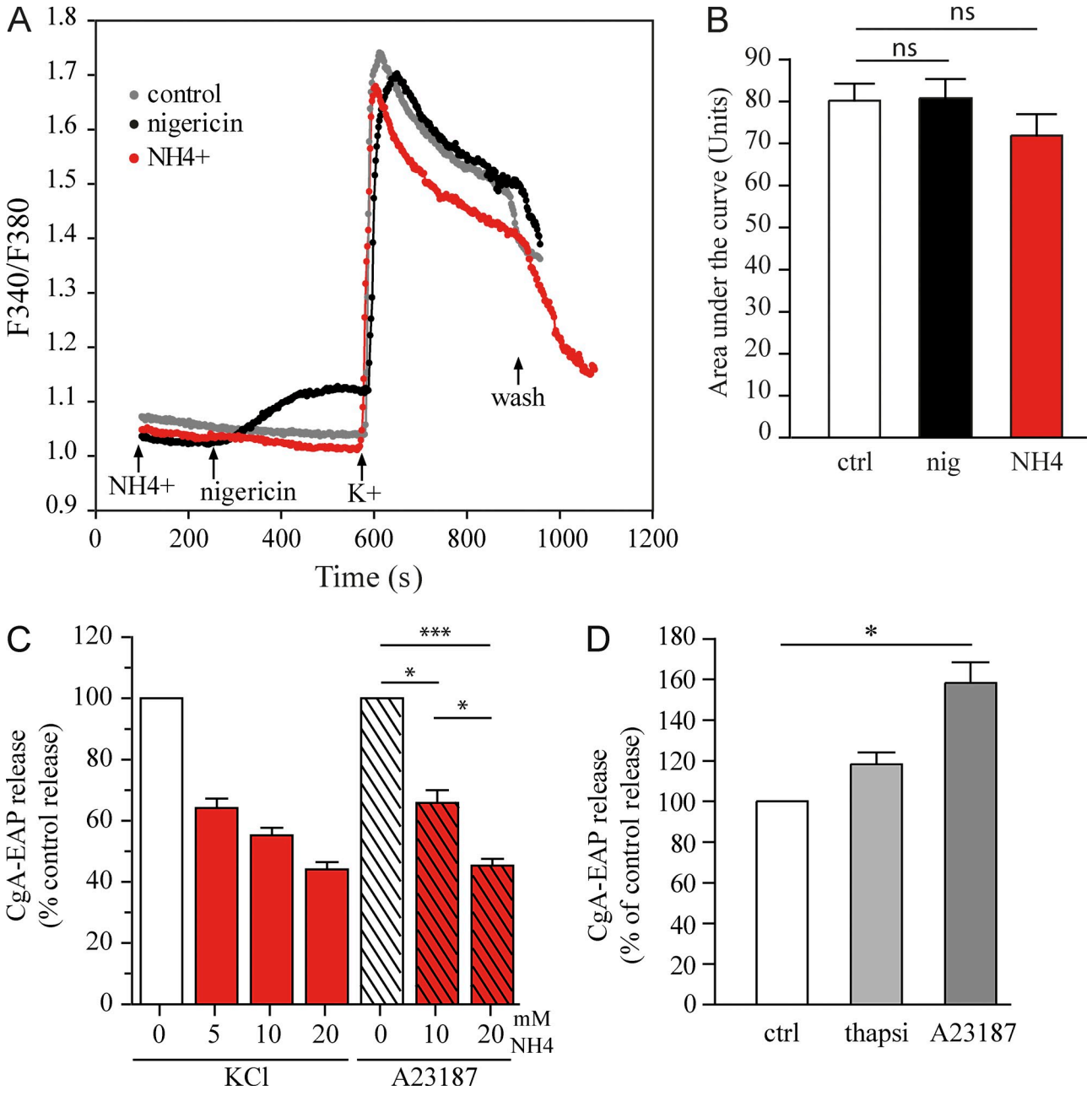

Figure 5. **Incubation with nigericin or 20 mM NH_4Cl does not affect exocytosis by impacting Ca^{2+} influx or calcium internal stores.** (A) PC12 cells loaded with Fura-2 were used to estimate variations of the cytosolic Ca^{2+} concentration. The basal Ca^{2+} concentration in the cytosol was not affected by the presence of 20 mM NH_4Cl. 5 µM nigericin elicited a progressive increase of cytosolic Ca^{2+} (probably from internal stores because no external Ca^{2+} was present). K^+ depolarization in the presence of 2 mM external calcium induced a marked increase of the cytosolic Ca^{2+} concentration, which was not much affected by nigericin or NH_4Cl. Curves are means from 38 or 39 cells from three to four independent experiments (for clarity, SDs that were always inferior to 10% of the means are not shown). (B) Quantification of the Fura-2 signals resulting from a 5-min-long K^+ depolarization, without (control [ctrl]) or in the presence of 5 µM nigericin (nig) or 20 mM NH_4Cl (NH4). Means ± SEM from 38 or 39 cells from three to four different cell cultures. (C) NH_4Cl (10 and 20 mM) similarly reduced CgA-EAP release induced by KCl depolarization or by the calcium ionophore A23187 (A23187) in the presence of 2 mM external calcium. Data are means ± SEM. (D) PC12 cells expressing CgA-EAP were preincubated 15 min with 10 µM thapsigargin (Thapsi) or with 10 µM calcium ionophore A23187 in the absence of external calcium before triggering CgA-EAP release by KCl. Data were obtained from four (A23187) or three (thapsigargin) different cell cultures. Data are means ± SEM. *, $P < 0.05$; ***, $P < 0.001$.

These results suggest that the intragranular pH regulates the dissociation of V1 from V0. Acidic pH, or bafilomycin A1 binding to V0, favors V1 dissociation, rendering V0 free for other protein interactions that might be important for the exocytotic machinery.

Discussion

Most of the standard cell biology approaches (e.g., RNA interference and dominant-negative mutants) are difficult to use to probe the function of V0 in exocytotic membrane fusion

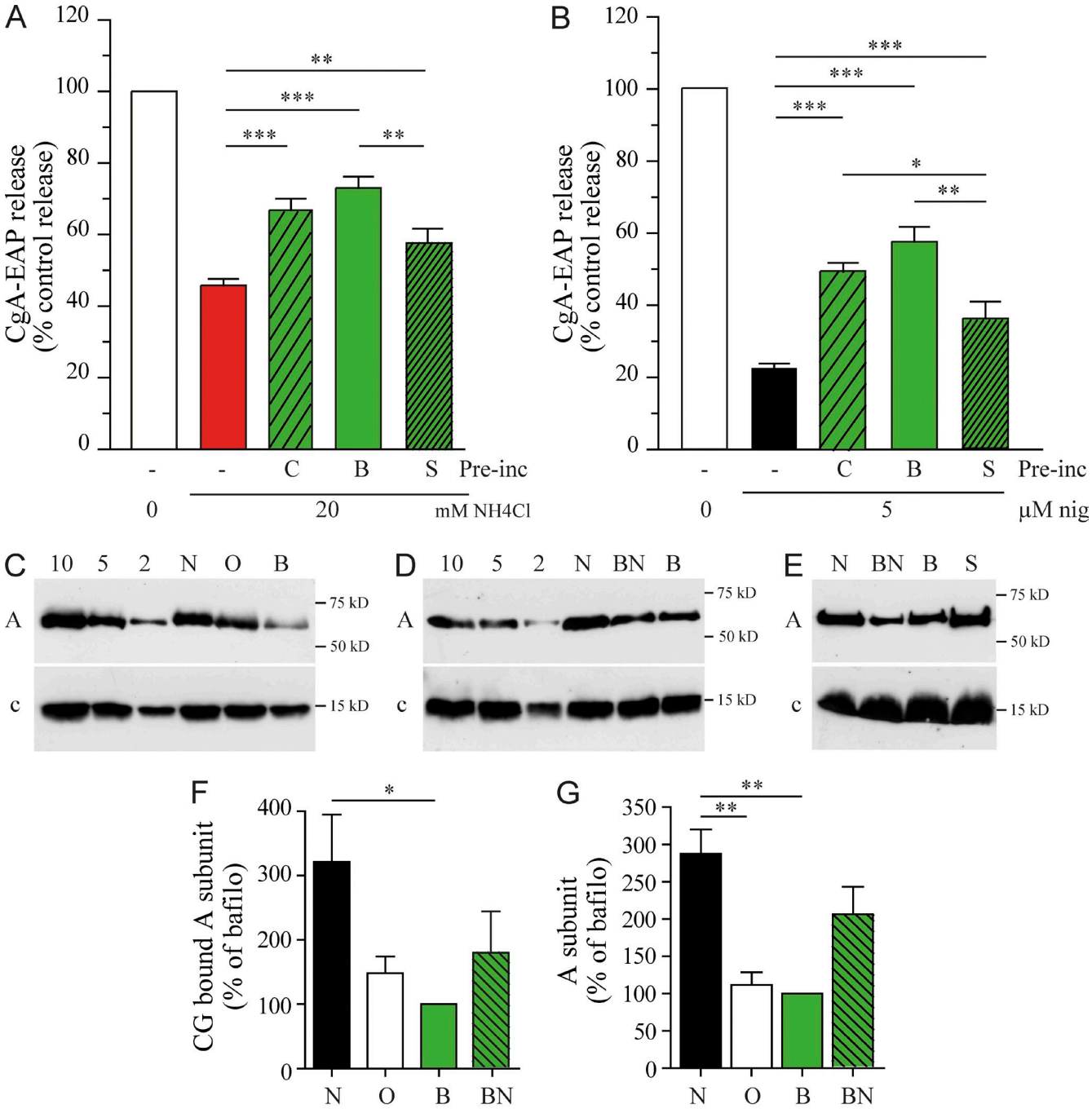

Figure 6. **V-ATPase association acts as a sensor of intragranular pH.** (A) CgA-EAP release after a 20-mM NH_4Cl incubation (45.9 ± 1.8% of control release, *n* = 31) was rescued by preincubation (Pre-inc) with 0.4 µM bafilomycin A1 (B; 73.1 ± 3.2%, *n* = 15) or concanamycin A (C; 66.9 ± 3.2%, *n* = 16). Protection by 0.4 µM saliphenylhalamide A (S) was less effective (57.6 ± 4.0%, *n* = 10). (B) CgA-EAP release after 5 µM nigericin (nig) incubation (22.5 ± 1.2% of control release, *n* = 29) was rescued by preincubation with 0.4 µM bafilomycin A1 (57.5 ± 4.1%, *n* = 9) or concanamycin A (49.5 ± 2.6%, *n* = 19). Saliphenylhalamide A was less effective (35.9 ± 4.7%, *n* = 8). (C) PC12 cells stably expressing CgA-EAP and Flag-TC-a1-I V0 subunit were incubated with 5 µM nigericin (N), 0.4 µM bafilomycin A1, or without treatment (0) for 15 min at 37°C. Cells were incubated with DSP to cross-link the V1–V0 domains before cell lysis and chromaffin granules isolation. The amount of V1 subunit A associated to granules (A) was estimated on Western blots, normalized at equivalent amounts of the endogenous V0 c subunit (c) or Flag a1-I (not depicted). Band intensities were quantified by comparison with increasing amounts of pooled granule fractions (2, 5, and 10). (D) Cells were preincubated for 30 min with 0.4 µM bafilomycin A1 before nigericin treatment (BN) or in physiological medium and then treated with 5 µM nigericin or bafilomycin A1 and treated as in C. (E) Cells treated with 0.4 µM saliphenylhalamide A and as described for D. (F and G) Quantification of the amount of V1 subunit A bound to chromaffin granules, normalized at constant V0 endogenous c subunit (F) or V0 Flag-a1-I subunit (G), expressed in the percentage of bafilomycin A1–treated samples (from three to five different experiments). Data are means ± SEM. *, P < 0.05; **, P < 0.01; ***, P < 0.001.

because of its ubiquitous and essential role in proton translocation, which is important for cell viability, many cellular processes, and required for secretory vesicle loading. Nevertheless, a direct additional role of V0 in exocytosis has been suggested after the observation that impairment of an organelle-specific isoform of the V0 a subunit generated exocytotic membrane fusion deficits that other subunit a isoforms were unable to rescue, whereas these subunit a isoforms were able to compensate for organelle acidification (Hiesinger et al., 2005; Liégeois et al., 2006). But it remained difficult to completely rule out indirect effects because other acidic compartments and membrane traffic events were affected in these experiments (Liégeois et al., 2006; Williamson et al., 2010). Hence, we have set up an acute and selective inactivation of V0 to bypass such limitations by using the CALI technology. This approach is known to allow acute and temporally controlled inactivation of a TC-tagged protein (Tour et al., 2003; Jacobson et al., 2008). Excitation of the chromophore FlAsH-EDT_2 bound to the TC motif leads to irreversible damage of the tagged protein. The destructive effects of CALI are mediated by a singlet oxygen within a radius of 3–50 nm (Tour et al., 2003; Yan et al., 2006) so that only the protein of interest is inactivated (Marek and Davis, 2002). This is especially evident in our results because the photoinactivation of two subunits within the same protein complex, the V0 a1-I or the V1 A subunits, led to clearly different functional alterations of synaptic transmission and granule exocytosis, in spite of the fact that the TC motifs were exposed to the cytosol in both cases.

The photoinactivation of the presynaptic V0 a1-I subunit in neurons resulted in a rapid and dramatic decrease of neurotransmitter release. Similarly, the inactivation of the chromaffin granule V0 a1-I subunit modified catecholamine release as shown by the decrease in exocytotic spike frequency. In these experiments, the recombinant TC-tagged a1-I subunit was estimated to be four to five times more abundant than the endogenous protein (Fig. S3), correctly addressed to the granules and able to rescue V-ATPase activity after silencing of the endogenous subunit (Fig. S4). Therefore, most of the V0 should contain the recombinant subunit and be inactivated. The fact that we observed no complete loss of neurotransmission or catecholamine release suggests that either the photoinactivation of V0 results in a partial loss of function or alternatively that V0 might be a modulator of the membrane fusion machinery (Di Giovanni et al., 2010).

Amperometric recordings have shown that the inactivation of a1-I affects the exocytotic spike frequency but also their kinetics, with a broadening of the spikes and shortening of the foot current duration. V0 inactivation therefore affects the fusion pore stability and slows down the membrane fusion process. Hence, V0 could participate in the organization of the fusion pore, possibly via V0–SNARE interactions (Galli et al., 1996; Morel et al., 2003; Hiesinger et al., 2005; Di Giovanni et al., 2010). V0 could also speed up membrane fusion by favoring lipid mixing between the interacting membranes (Strasser et al., 2011) and the expansion of the fusion pore. In agreement with the later hypothesis, V0 contains a hexameric proteolipid ring made of very hydrophobic subunits that are soluble in organic solvents (Israël et al., 1986), and mutations impairing lipid mixing were identified in these subunits (Strasser et al., 2011).

The role of V0 on secretory vesicle exocytosis is independent of proton transport because the photoinactivation of the V1 catalytic A subunit or the blockade of proton transport by bafilomycin A1 did not affect exocytosis itself but only led to a delayed decrease of the granule catecholamine content resulting from the progressive dissipation of the granular pH gradient (Fig. 3) and catecholamine leakage into the cytosol (Camacho et al., 2006). Nevertheless, independently of proton transport itself, the intragranular pH might be important for exocytosis as shown in several different organelle traffic events (Kuijpers et al., 1989; Ungermann et al., 1999; Barg et al., 2001; Camacho et al., 2006; but see Cousin and Nicholls, 1997). Using CgA-EAP release as a marker for granule exocytosis, we found that nigericin or NH_4Cl treatments inhibited exocytosis, whereas CgA-EAP granule content was unaffected. This inhibition was not caused by a modification of the influx of Ca^{2+} through voltage-dependent calcium channels and intracellular Ca^{2+} levels during depolarization (Fig. 5, A and B), nor to an alteration of internal calcium stores (Fig. 5 D), or to an altered mitochondrial ATP synthesis (Fig. S5). The cytosolic pH, which was not modified after incubation with bafilomycin A1 and slightly raised after NH_4Cl or nigericin treatments (unpublished data), remained within a physiological range that does not affect exocytosis (Thomas et al., 1993; Lindgren et al., 1997). Therefore, granule exocytosis impairment after NH_4Cl or nigericin treatments appeared to be directly related to the rise in the intragranular pH, an efficient exocytosis requiring acidic granules. We propose that the intragranular pH regulates the exocytotic machinery by inducing V0 conformational changes. At acidic intragranular pH, V0 would be in a fusion-permissive conformation that favors exocytosis. In addition, bafilomycin A1 or concanamycin A binding to V0 would stabilize this fusion-permissive conformation, both inhibitors sharing the same binding site on V0 (Bowman et al., 2006). This would explain why inhibiting the V-ATPase activity with bafilomycin A1 or concanamycin A dissipated the granular pH gradient without affecting exocytosis, whereas saliphenylhalamide A, which binds to a different site on V0 (Xie et al., 2004), affected both the granular pH and exocytosis. This would also explain why a preincubation with bafilomycin A1 or concanamycin A partially protected exocytosis from the inhibition caused by NH_4Cl or nigericin (Fig. 6). At acidic pH, or after binding of bafilomycin A1, V0 appeared to be in a conformation that favors the dissociation of the catalytic V1 domain, whereas, at neutral pH, V0 is in association with V1 (Fig. 6). Similarly, the alkalization of yeast vacuoles has previously been shown to increase V1 association (Shao and Forgac, 2004). Saliphenylhalamide A, in contrast to bafilomycin A1, increased the V0–V1 association (Fig. 6), as previously reported with its analogue salicylihalamide A (Xie et al., 2004). This strongly suggests that what accounts for the reduced exocytosis is a conformational state of V0 after bafilomycin A1 binding, rather than the inhibition of V-ATPase activity. Mutagenesis of yeast vacuole V0 proteolipid subunits identified amino acids that are important for membrane fusion (Strasser et al., 2011), some of them being part of the bafilomycin A1 binding site (Bowman et al., 2006).

The identified mutations were also shown to modify the association of V0 with V1 (Strasser et al., 2011). Reversible dissociation of the V1 and V0 V-ATPase domains occurs in various physiological situations as a means to regulate the enzymatic activity (Forgac, 2007; Toei et al., 2010). Upon V-ATPase dissociation, the V1 subunit C is released and V1 (minus subunit C) is detached from V0; their reassociation to V0 is an energy consuming process that requires the cytosolic RAVE (regulator of the H^+-ATPase of the vacuolar and endosomal membranes) protein complex (Smardon and Kane, 2007). Recent structural data suggested that the insertion of subunit C within the V1–V0 complex requires "spring loading" structural constraints (Oot et al., 2012). Inversely, a minor structural deformation transmitted to subunit C should be sufficient to dissociate V1 (Stewart and Stock, 2012). The V0 subunit a, which interacts with subunit C via its cytoplasmic domain (Oot and Wilkens, 2012), is a good candidate to link intragranular pH changes and conformational changes of the proteolipid subunits to the V1–V0 subunit C interface.

The dissociation of V1 renders V0 free to interact with other proteins. This could allow the recruitment of ARNO (ADP ribosylation factor nucleotide-binding site opener; cytohesin-2) and the GTPase Arf6 to the membrane by the V-ATPase, which has been proposed as a sensing mechanism of endosomal pH (Hurtado-Lorenzo et al., 2006; Hosokawa et al., 2013). Interestingly, Arf6 has been shown to modulate exocytosis in various cellular models, including chromaffin cells, mainly through the production of fusogenic lipids (Vitale et al., 2002; Aikawa and Martin, 2003; Bader and Vitale, 2009; Béglé et al., 2009). The possibility that the association/dissociation of V0–V1 also contributes in part to the regulation of fusogenic lipid synthesis through the ARNO–Arf6–PLD pathway remains, however, to be established. V0 has also been shown to interact with SNAREs. The association of V0 with the v-SNARE VAMP-2 occurs probably as a cis-complex within the same neurosecretory vesicles (Galli et al., 1996; Morel et al., 2003; Di Giovanni et al., 2010). Because this V0–VAMP-2 interaction persists when VAMP-2 is engaged in a SNARE complex (Morel et al., 2003), the V0–VAMP-2 complex could remain operative during the late steps of membrane fusion. An interaction of V0 with the t-SNARE syntaxin-1 has also been reported (Hiesinger et al., 2005). It is probably not relevant as an intravesicular pH sensing mechanism because it involves either a trans-interaction between a vesicular V0 and syntaxin-1 in the presynaptic membrane and, therefore, concerns a limited number of already docked synaptic vesicles or a cis-interaction within the presynaptic plasma membrane, unrelated to secretory vesicles, because V0 is also present within the nerve terminal plasma membrane (Morel et al., 2003). It should be stressed here that only one or two molecules of V-ATPase are present per synaptic vesicle (Hicks and Parsons, 1992) as compared with ∼30 VAMP-2 molecules (Takamori et al., 2006). This places these one or two V0 molecules in a strategic position. The role of V0 in sensing the intravesicular pH probably concerns a priming step that confers to secretory granules the competence for release, before the formation of trans-SNARE complexes (Ungermann et al., 1999; Barg et al., 2001). The role of V0 in controlling fusion pore stability and membrane lipid mixing, based on yeast vacuole fusion experiments, should occur after trans-SNARE pairing (Peters et al., 2001; Strasser et al., 2011).

Estimates of the amount of transmitter released by single exocytotic events and of the size of vesicles suggest that, in accordance with the quantal hypothesis, fully loaded vesicles are released in preference to partially filled ones (Albillos et al., 1997; Bruns et al., 2000; Tabares et al., 2001). Because in many synapses postsynaptic receptors are not saturated by the released neurotransmitter, the control of the neurotransmitter content of synaptic vesicles is critical for neuronal function (Edwards, 2007). As previously discussed (Edwards, 2007), synaptic vesicle exocytosis does not appear to be influenced by the inhibition of vesicular neurotransmitter transporters and therefore by the vesicular neurotransmitter concentration. Sensing the loading status of synaptic vesicles might therefore rely on V-ATPase conformational changes in response to variations of the intravesicular pH. The V0 domain might be of decisive importance in signaling to the exocytotic machinery if a synaptic vesicle is undergoing neurotransmitter reloading (i.e., consuming its pH gradient) or if it is fully loaded (i.e., acidic) and ready to be released into the synaptic cleft (Morel, 2003).

Materials and methods

Reagents

The following reagents were obtained from Sigma-Aldrich: bafilomycin A1, concanamycin A, oligomycin A, valinomycin, thapsigargin, ionophore A23187, BAL, and proteases inhibitor cocktail (P8340). Nigericin was obtained from Tocris Bioscience. Saliphenylhalamide was a gift from J.K. De Brabander (University of Texas Southwestern Medical Center, Dallas, TX). FlAsH-EDT_2 was purchased from Invitrogen or had been synthesized for us by Orga-Link according to Adams and Tsien (2008). Antibodies to rat V0 c subunit were a generous gift from S. Okhuma (Kanazawa University, Kanazawa, Japan). Affinity-purified antibodies to the V1 A and V0 a1 subunits were prepared in the laboratory as previously described (Morel et al., 2003; Poëa-Guyon et al., 2006). In brief, antisera were raised in rabbits by immunization with peptides corresponding to C-terminal epitopes (EDMQNAFRSLED for V1 A and FSFEHIREGKFDE for V0 a1) linked to the carrier protein KLH via an added K (V1 A) or C (V0 a1) in the N-terminal position. Antibodies were then affinity purified on the corresponding peptides linked to Sepharose beads (UltraLink Iodoacetyl or SulfoLink gels obtained from Thermo Fisher Scientific for V1 A and V0 a1, respectively) according to manufacturer's instructions. Anti-Flag and anti-EAP antibodies were from Sigma-Aldrich and EMD Millipore, respectively. DSP was obtained from Thermo Fisher Scientific. Fura-2–acetoxymethyl (AM) and BCECF-AM were purchased from Invitrogen and Molecular Probes, respectively.

Plasmids

The following plasmids were used to direct the expression of recombinant proteins. All inserted coding sequences and the junctions with the vectors were verified by sequencing. Plasmids p104, p165, and p166 contain the coding sequences for Flag-TC-a1-I, a1-I-TC-Flag, and Flag-TC-A, respectively, inserted in the pIRES–humanized recombinant-GFP 1a bicistronic expression vector (Agilent Technologies) and direct the coexpression of the recombinant proteins and of EGFP. In all cases, the sequence encoding the TC tag (peptide FLNCCPGCCMEP containing the tetracysteine motif; Martin et al., 2005) was inserted by restriction between the Flag tag and the subunit sequence. Plasmid pcDNA6-CgA-EAP, obtained from L. Taupenot (University of California, San Diego, La Jolla, CA; Taupenot et al., 2005), was used to generate PC12 cell clones that stably express CgA-EAP. Plasmid p95 contains the Flag-TC-a1-I coding sequence inserted in the p3×Flag-CMV26 vector (Sigma-Aldrich) that confers resistance to the antibiotic G418.

Photoinactivation of the V0 a1-I subunit and synaptic transmission

Primary cultures of rat hippocampal neurons or mouse cortical neurons were performed essentially as described previously (Goslin et al., 1998;

Poëa-Guyon et al., 2006). Hippocampi and cortex sections of 18- and 17-d-old rat and mouse embryos, respectively, were removed and mechanically dissociated after a mild trypsin digestion. For rat cultures, cells were plated onto poly-L-lysine–coated glass coverslips and allowed to settle for 2 h. They were then transferred onto a glial cell monolayer in the Neurobasal medium supplemented with B27 (Invitrogen). For mouse cells, neurons were directly plated on polyornithine-coated glass coverslips in culture medium containing bovine fetal serum. Proliferation of nonneuronal cells was prevented by addition, 1 d after plating, of cytosine arabinoside (5-µM final concentration). Neurons were transfected at 7 d in vitro with the indicated plasmids using Lipofectamine 2000 (Invitrogen) according to the manufacturer's instructions. They were used 7–12 d after transfection. Coverslips containing transfected and untransfected neurons were transferred to a recording chamber and continuously perfused with a bubbled (95% O_2/5% CO_2) artificial cerebrospinal fluid containing (mM): 126 NaCl, 26 $NaHCO_3$, 10 glucose, 2 $CaCl_2$, 1.5 KCl, 1.5 $MgSO_4$, and 1.25 KH_2PO_4, pH 7.5 (310–320 mOsm at 37°C). Stable whole-cell pair recordings were obtained under video-enhanced differential interference contrast using an upright microscope (Axioskop 2 FS+; Carl Zeiss). Patch pipettes (of 5–7 MΩ resistance) contained the following intracellular solution (mM): 140 K-gluconate, 10 Hepes, 4 ATP, 2 $MgCl_2$, 0.4 GTP, and 0.5 EGTA, pH 7.3 (adjusted with KOH; 280–290 mOsm). A single action potential was elicited in transfected neurons expressing GFP (by a brief depolarizing step under current clamp) to generate a postsynaptic response in a neighboring untransfected neuron (recorded under voltage clamp). Synaptically connected neurons were exposed to 1 µM FlAsH-EDT_2 (diluted in O_2/CO_2-saturated artificial cerebrospinal fluid) for 10 min. Then, neurons were perfused with 1 mM BAL. Finally, whole-field illumination was achieved through the microscope 40× objective for 1 min to allow the photoinactivation of the TC-tagged V-ATPase subunits (light was delivered by a 120-W xenon lamp [X-Cite 120Q; Exfo] via an optical fiber). Presynaptic action potentials and postsynaptic currents were continuously monitored, before and after the photoinactivating flash. Postsynaptic responses were expressed as a percentage of the mean amplitude of postsynaptic currents recorded during the 5 min preceding the flash. Only neuronal pairs showing stable baseline before flash and changes in resting membrane potential inferior to 25% were kept for analysis.

Photoinactivation of V0 a1-I and V1 A subunits and catecholamine release

Freshly dissected primary bovine chromaffin cells were cultured in DMEM in the presence of 10% fetal calf serum, 10 µM cytosine arabinoside, 10 µM fluorodeoxyuridine, and antibiotics as described previously (Vitale et al., 1993). Bicistronic plasmids expressing V-ATPase subunits and GFP were introduced into chromaffin cells (5×10^6 cells) by transfection systems (Amaxa Nucleofector; Lonza) according to manufacturer's instructions. 48/72 h after transfection, cells were exposed to 1 µM FlAsH-EDT_2 in Locke's buffer for 10 min and subsequently incubated with 1 mM BAL for 10 min. Locke's buffer is composed of 140 mM NaCl, 4.7 mM KCl, 2.5 mM $CaCl_2$, 1.2 mM $MgSO_4$, 15 mM Hepes, and 11 mM glucose, pH 7.4. Medium was replaced with Locke's buffer before a 1-min illumination through the microscope setup using a high power light-emitting diode (BLCC-2; Prizmatix). Catecholamine secretion was evoked by applying 100 mM K^+ in Locke's solution without ascorbic acid for 10 s to single cells by means of a glass micropipette positioned at a distance of 30–50 µm from the cell. Electrochemical measurements of catecholamine secretion were performed using 5-µm-diameter carbon fiber electrodes (ALA Scientific Instruments) held at a potential of 650 mV compared with the reference electrode (Ag/AgCl) and approached closely to the transfected cells essentially as described previously (Chasserot-Golaz et al., 2005). Amperometric recordings were performed with an amplifier (AMU130; Radiometer Analytical), sampled at 5 kHz, and digitally low pass filtered at 1 kHz. Analysis of amperometric recordings was performed with a macro (obtained and freely available from R. Borges laboratory [Analysis program 3.3]) written for Igor software (WaveMetrics), allowing automatic spike detection and extraction of spike parameters (Segura et al., 2000). The number of amperometric spikes was counted as the total number of spikes with an amplitude >5 pA.

Generation of PC12 cell lines and CgA-EAP exocytosis measurements

PC12 cells were transfected with the plasmid pcDNA6-CgA-EAP 48 h before selection for blasticidin S resistance (essentially as in Taupenot et al., 2005). PC12 cells were cultivated in high glucose DMEM containing L-glutamine (Invitrogen) with 10% horse serum (Sigma-Aldrich), 5% fetal bovine serum (Biowest), penicillin, and streptomycin (Invitrogen). Cells, seeded on rat tail collagen type I (Jacques Boy Institute)–coated plastic dishes (10 µg/cm^2), were transfected with the plasmid pcDNA6-CgA-EAP (Lipofectamine 2000; Invitrogen). Blasticidin S–resistant PC12 colonies were selected with cloning rings and further grown in 24-well collagen-coated culture plates, in the continuous presence of 10 µg/ml blasticidin S. Clones were screened for regulated CgA-EAP release by chemiluminescence. The 2B2 cell line was selected and used throughout this work. It was also transfected with plasmid p95 that confers resistance to 0.5 mg/ml Geneticin G418 to generate the 2B2-95 cell line that stably expresses CgA-EAP together with the Flag-TC-a1-I V0 subunit. Detection of EAP activity release from CgA-EAP–expressing PC12 cells was achieved by chemiluminescence using the Phospha-Light assay (Roche; Applied Biosystems), according to manufacturer's instructions, in a microplate luminometer (Mithras; Berthold). In brief, cells were grown in collagen-coated 24-well culture plates for 48 h to 60–90% confluency. They were incubated at 37°C in 300 µl/well of the physiological medium M (128 mM NaCl, 5 mM KCl, 1 mM $MgCl_2$, 1 g/liter glucose, 10 mM Hepes, 10 mM $NaHCO_3$, and 2 mM NaH_2PO_4, pH 7.35) with or without drugs as indicated. Basal release was measured at 37°C in 150 µl/well of medium M after a 5- or 15-min incubation. Evoked release was measured after a 5- or 15-min incubation at 37°C in the stimulation medium S (63 mM NaCl, 70 mM KCl, 2 mM $CaCl_2$, 1 mM $MgCl_2$, 1 g/liter glucose, 10 mM Hepes, 10 mM $NaHCO_3$, and 2 mM NaH_2PO_4, pH 7.35). In these conditions, 2B2 and 2B2-95 cells displayed a 10-fold increase in CgA-EAP release after cell depolarization. CgA-EAP release (measured in triplicate) was expressed as a percentage of total EAP activity within the cells before stimulation. Total cellular EAP activity is the sum of the released EAP activity plus the activity remaining in the cells (measured after 0.2% Triton X-100 addition). It was not affected by the various pharmacological treatments used in this work.

FLIM of intragranular pH

ECFP was amplified by high fidelity PCR from the pECFP-N1 vector (Takara Bio Inc.) with a forward primer designed to introduce a KpnI restriction site just before the initial ATG and a reverse primer introducing the NotI restriction site just downstream from the TAA stop codon. The amplified ECFP sequence was inserted into the pcDNA6-CgA-EAP vector (see Plasmids) in place of the EAP coding sequence using the KpnI–NotI restriction sites. 2B2 or 2B2-95 PC12 cells, cultured on poly-L-ornithine–coated glass slides, were transfected with the CgA-ECFP–encoding vector using Lipofectamine 2000 (10 µg DNA/25 µl Lipofectamine 2000), and experiments were performed 48 h after transfection. PC12 cells were incubated at 36 ± 2°C in the physiological medium M with or without 5 µM nigericin, NH_4Cl (5, 10, or 20 mM in place of equivalent amounts of NaCl), or 0.4 µM V-ATPase inhibitors (bafilomycin A1, concanamycin A, or saliphenylhalamide A). For pH calibration, cells were incubated in buffers containing 15 mM MES, 15 mM Hepes, 140 mM KCl, and 10 µM nigericin at pH ranging from 5 to 7.5. Time-resolved, laser-scanning, time-correlated single photon counting microscopy was performed on a homemade setup based on a microscope (TE2000; Nikon) equipped with a 60×, 1.2 NA water immersion objective and a fiber-coupled scanning head (C1; Nikon) already previously described in detail elsewhere (Erard et al., 2013). The FLIM setup allows real-time monitoring of ECFP lifetime variations and provides highly reproducible results (Poëa-Guyon et al., 2013).

Fura-2 imaging

Cells plated on polyornithine-coated coverslips were loaded with 5 µM Fura-2–AM in HBSS for 30 min (37°C) and rinsed for 10 min with fresh culture medium (DMEM containing 10% fetal bovine serum). Coverslips were mounted in a perfusion chamber in medium M (see Generation of PC12 cell lines and CgA-EAP exocytosis measurements) before imaging with a videomicroscope (DMI6000; Leica) fitted with a high-speed filter changer (Lambda DG-4; Sutter Instrument) to rapidly change excitation between 340 and 380 nm, and fluorescence emission was collected at 510 nm by a band pass filter. Acquisition of fluorescence and image analysis were performed using a digital imaging system (SimplePCI; Hamamatsu Photonics). The fluorescence ratios for 340- and 380-nm excitations (R340/380) were measured at 2-s intervals during perfusion with medium M, alone or with 5 µM nigericin, 0.4 µM bafilomycin A1, or 20 mM NH_4Cl and after switching to the stimulation medium S (with or without the drugs) for 5 min.

BCECF imaging

The intracellular pH of PC12 cells was determined using BCECF according to the manufacturer's instructions (Invitrogen). In brief, plated cells were incubated for 1 h (at RT) in HBSS containing 2 µM BCECF-AM and rinsed for 1 h with fresh culture medium (at 37°C). Coverslips were mounted in the perfusion chamber as described for Fura-2 imaging in the videomicroscope

(excitation filters were 440AF21 for 440 nm and 490DF20 for 490 nm and the emission filter was 535DF25). The fluorescence ratios for 490- and 440-nm excitations ($R_{490/440}$) were measured at 20-s intervals. For cytosolic pH calibration, cells were perfused with 10 µM nigericin-containing buffers (see FLIM of intragranular pH), and $R_{490/440}$ was determined at five different pH values (between 6.8 and 7.6).

Association of the V1 A subunit to secretory granules

The 2B2-95 PC12 cells were grown in 75-cm^2 collagen-coated culture flasks to ∼70–90% confluency. They were washed with 10 ml of medium M (see Generation of PC12 cell lines and CgA-EAP exocytosis measurements) and incubated with the indicated drugs in medium M for 15 min at 37°C. V1–V0 cross-linking (Morel et al., 1998) was then performed at 20–22°C for 30 min in the presence of the various drugs in medium M that also contained 1 mM DSP (from a freshly prepared 0.6 M solution in DMSO). Unreacted DSP was then quenched by the addition in the culture flasks of 0.5 ml of 0.5-M Tris buffer, pH 7.5 (25-mM final concentration), for 15 min at 20–22°C. Cells were then harvested by scraping the flasks and pelleting the cells (800 g_{max} for 10 min). Cells were resuspended in 2 ml (for cells from a 75-cm^2 flask) of the fractionation medium F (300 mM sucrose, 1 mM EGTA, and 10 mM Tris buffer, final pH 7.4) supplemented with a mix of protease inhibitors (Sigma-Aldrich). They were disrupted in a cell homogenizer (16-µm clearance bead; Isobiotec). The lysate was centrifuged (800 g_{max} for 10 min). The supernatant was layered on top of a semicontinuous sucrose gradient made of four layers that were allowed to diffuse (1.5 ml of 1.4-, 1.2-, and 1.0-M sucrose and 3 ml of 0.8-M sucrose in 1 mM EGTA and 10 mM Tris buffer, final pH 7.4). After centrifugation (40,000 rpm for 120 min in the rotor [SW 41; Beckman Coulter]), 0.5-ml fractions were collected and tested for CgA-EAP activity by chemiluminescence and sucrose concentration by refractometry. The granule-containing fractions, identified as a peak of EAP activity at ∼1.2 M sucrose, were pooled and diluted in medium F, and granules were pelleted (45,000 rpm for 60 min on a rotor [TI50; Beckman Coulter]). Granule-containing pellets were resuspended in the SDS-lysis buffer (containing 5% 2-mercaptoethanol) and heated at 95°C for 5 min. Proteins were separated by electrophoresis in 5–15% acrylamide gradient gels and electroblotted onto nitrocellulose, and blots were probed with anti-A, anti-c, or anti-Flag antibodies. Immunoreactive bands were visualized after secondary peroxidase-conjugated antibody binding by chemiluminescence (SuperSignal West Pico or Dura; Thermo Fisher Scientific). Band luminescence was captured in an imager (GeneGnome; Syngene Bio Imaging) and quantified using the GeneSnap software (Syngene Bio Imaging).

Immunostaining and imaging

Cells were fixed with 4% paraformaldehyde and labeled with a rabbit polyclonal anti-Flag antibody (Sigma-Aldrich) and FITC-labeled goat anti–rabbit antibody (Molecular Probes) or a mouse monoclonal anti-EAP antibody (EMD Millipore) and Alexa Fluor 568–labeled goat anti–mouse antibody (Molecular Probes). Images were acquired using a confocal microscope (LSM 700; Carl Zeiss) with Plan Apochromat 63×/1.4 NA oil immersion objective lenses and ZEN (Carl Zeiss) as the image acquisition software. All images were taken at RT. Images for figures were processed with ImageJ software (National Institutes of Health) to enhance brightness using the brightness/contrast function and smoothened (0.5-pixel σ radius) using the Gaussian blur function.

Statistical analysis

Data are presented as mean values ± SEM. Statistical comparisons (Student's *t* test) were performed with the Prism 4 software (GraphPad Software). Significant differences were marked *, $P < 0.05$; **, $P < 0.01$; and ***, $P < 0.001$.

Online supplemental material

Fig. S1 shows that the insertion of the Flag-TC tags does not affect targeting of a1-I or A subunits to secretory granules in PC12 cells. Fig. S2 shows that photoinactivation of the neuronal a1-I V0 subunit impairs neurotransmitter release independently from V-ATPase proton transport. Fig. S3 shows relative amounts of recombinant Flag-TC–tagged a1-I and endogenous a1 subunits in transfected PC12 cells. Fig. S4 shows that overexpression of a siRNA-resistant TC-a1-I construct rescues catecholamine release defects after V0 a1 silencing. Fig. S5 shows that CgA-EAP release is only slightly inhibited by the mitochondrial F1F0-ATPase inhibitor oligomycin A. Table S1 shows the effect of CALI treatment and V-ATPase subunit overexpression on catecholamine release from chromaffin cells. Online supplemental material is available at http://www.jcb.org/cgi/content/full/jcb.201303104/DC1.

We thank V. Rousseau and Dr. J.-V. Barnier for help on the videomicroscope setup used for Fura-2 and BCECF imaging, Dr. S. O'Reagan for improving our manuscript, Dr. L. Taupenot for the pcDNA6-CgA-EAP plasmid, T. Thahouly for chromaffin cell culture, and Dr. De Brabander for providing us with saliphenylhalamide A.

This work was supported by the Agence Nationale pour la Recherche (grant ANR-09-blan-0264-04 to N. Vitale and N. Morel).

Submitted: 20 March 2013
Accepted: 19 September 2013

References

Adams, S.R., and R.Y. Tsien. 2008. Preparation of the membrane-permeant biarsenicals FlAsH-EDT2 and ReAsH-EDT2 for fluorescent labeling of tetracysteine-tagged proteins. *Nat. Protoc.* 3:1527–1534. http://dx.doi.org/10.1038/nprot.2008.144

Aikawa, Y., and T.F. Martin. 2003. ARF6 regulates a plasma membrane pool of phosphatidylinositol(4,5)bisphosphate required for regulated exocytosis. *J. Cell Biol.* 162:647–659. http://dx.doi.org/10.1083/jcb.200212142

Albillos, A., G. Dernick, H. Horstmann, W. Almers, G. Alvarez de Toledo, and M. Lindau. 1997. The exocytotic event in chromaffin cells revealed by patch amperometry. *Nature*. 389:509–512. http://dx.doi.org/10.1038/39081

Bader, M.F., and N. Vitale. 2009. Phospholipase D in calcium-regulated exocytosis: lessons from chromaffin cells. *Biochim. Biophys. Acta*. 1791:936–941. http://dx.doi.org/10.1016/j.bbalip.2009.02.016

Barg, S., P. Huang, L. Eliasson, D.J. Nelson, S. Obermüller, P. Rorsman, F. Thévenod, and E. Renström. 2001. Priming of insulin granules for exocytosis by granular Cl(-) uptake and acidification. *J. Cell Sci.* 114: 2145–2154.

Béglé, A., P. Tryoen-Tóth, J. de Barry, M.F. Bader, and N. Vitale. 2009. ARF6 regulates the synthesis of fusogenic lipids for calcium-regulated exocytosis in neuroendocrine cells. *J. Biol. Chem.* 284:4836–4845. http://dx.doi.org/10.1074/jbc.M806894200

Bowman, B.J., M.E. McCall, R. Baertsch, and E.J. Bowman. 2006. A model for the proteolipid ring and bafilomycin/concanamycin-binding site in the vacuolar ATPase of *Neurospora crassa*. *J. Biol. Chem.* 281:31885–31893. http://dx.doi.org/10.1074/jbc.M605532200

Bruns, D., D. Riedel, J. Klingauf, and R. Jahn. 2000. Quantal release of serotonin. *Neuron*. 28:205–220. http://dx.doi.org/10.1016/S0896-6273(00)00097-0

Camacho, M., J.D. Machado, M.S. Montesinos, M. Criado, and R. Borges. 2006. Intragranular pH rapidly modulates exocytosis in adrenal chromaffin cells. *J. Neurochem.* 96:324–334. http://dx.doi.org/10.1111/j.1471-4159.2005.03526.x

Cavelier, P., and D. Attwell. 2007. Neurotransmitter depletion by bafilomycin is promoted by vesicle turnover. *Neurosci. Lett.* 412:95–100. http://dx.doi.org/10.1016/j.neulet.2006.10.040

Chasserot-Golaz, S., N. Vitale, E. Umbrecht-Jenck, D. Knight, V. Gerke, and M.F. Bader. 2005. Annexin 2 promotes the formation of lipid microdomains required for calcium-regulated exocytosis of dense-core vesicles. *Mol. Biol. Cell*. 16:1108–1119. http://dx.doi.org/10.1091/mbc.E04-07-0627

Cousin, M.A., and D.G. Nicholls. 1997. Synaptic vesicle recycling in cultured cerebellar granule cells: role of vesicular acidification and refilling. *J. Neurochem.* 69:1927–1935. http://dx.doi.org/10.1046/j.1471-4159.1997.69051927.x

Di Giovanni, J., S. Boudkkazi, S. Mochida, A. Bialowas, N. Samari, C. Lévêque, F. Youssouf, A. Brechet, C. Iborra, Y. Maulet, et al. 2010. V-ATPase membrane sector associates with synaptobrevin to modulate neurotransmitter release. *Neuron*. 67:268–279. http://dx.doi.org/10.1016/j.neuron.2010.06.024

Edwards, R.H. 2007. The neurotransmitter cycle and quantal size. *Neuron*. 55:835–858. http://dx.doi.org/10.1016/j.neuron.2007.09.001

El Far, O., and M. Seagar. 2011. A role for V-ATPase subunits in synaptic vesicle fusion? *J. Neurochem.* 117:603–612.

Erard, M., A. Fredj, H. Pasquier, D.B. Beltolngar, Y. Bousmah, V. Derrien, P. Vincent, and F. Merola. 2013. Minimum set of mutations needed to optimize cyan fluorescent proteins for live cell imaging. *Mol. Biosyst.* 9:258–267. http://dx.doi.org/10.1039/c2mb25303h

Forgac, M. 2007. Vacuolar ATPases: rotary proton pumps in physiology and pathophysiology. *Nat. Rev. Mol. Cell Biol.* 8:917–929. http://dx.doi.org/10.1038/nrm2272

Füldner, H.H., and H. Stadler. 1982. 31P-NMR analysis of synaptic vesicles. Status of ATP and internal pH. *Eur. J. Biochem.* 121:519–524. http://dx.doi.org/10.1111/j.1432-1033.1982.tb05817.x

Galli, T., P.S. McPherson, and P. De Camilli. 1996. The V0 sector of the V-ATPase, synaptobrevin, and synaptophysin are associated on synaptic vesicles in a Triton X-100-resistant, freeze-thawing sensitive, complex. *J. Biol. Chem.* 271:2193–2198. http://dx.doi.org/10.1074/jbc.271.4.2193

Goslin, K., H. Asmussen, and G. Banker. 1998. Rat hippocampal neurons in low-density culture. *In* Culturing Nerve Cells. Second edition. G. Banker and K. Goslin, editors. MIT Press, Cambridge, MA. 339–370.

Hicks, B.W., and S.M. Parsons. 1992. Characterization of the P-type and V-type ATPases of cholinergic synaptic vesicles and coupling of nucleotide hydrolysis to acetylcholine transport. *J. Neurochem.* 58:1211–1220. http://dx.doi.org/10.1111/j.1471-4159.1992.tb11331.x

Hiesinger, P.R., A. Fayyazuddin, S.Q. Mehta, T. Rosenmund, K.L. Schulze, R.G. Zhai, P. Verstreken, Y. Cao, Y. Zhou, J. Kunz, and H.J. Bellen. 2005. The v-ATPase V0 subunit a1 is required for a late step in synaptic vesicle exocytosis in *Drosophila*. *Cell*. 121:607–620. http://dx.doi.org/10.1016/j.cell.2005.03.012

Hong, S.J. 2001. Reduction of quantal size and inhibition of neuromuscular transmission by bafilomycin A. *Neuropharmacology*. 41:609–617. http://dx.doi.org/10.1016/S0028-3908(01)00104-6

Hosokawa, H., P.V. Dip, M. Merkulova, A. Bakulina, Z. Zhuang, A. Khatri, X. Jian, S.M. Keating, S.A. Bueler, J.L. Rubinstein, et al. 2013. The N-termini of a-subunit isoforms are involved in signaling between vacuolar H+-ATPase (V-ATPase) and cytohesin-2. *J. Biol. Chem.* 288:5896–5913. http://dx.doi.org/10.1074/jbc.M112.409169

Hurtado-Lorenzo, A., M. Skinner, J. El Annan, M. Futai, G.H. Sun-Wada, S. Bourgoin, J. Casanova, A. Wildeman, S. Bechoua, D.A. Ausiello, et al. 2006. V-ATPase interacts with ARNO and Arf6 in early endosomes and regulates the protein degradative pathway. *Nat. Cell Biol.* 8:124–136. http://dx.doi.org/10.1038/ncb1348

Israël, M., N. Morel, B. Lesbats, S. Birman, and R. Manaranche. 1986. Purification of a presynaptic membrane protein that mediates a calcium-dependent translocation of acetylcholine. *Proc. Natl. Acad. Sci. USA*. 83:9226–9230. http://dx.doi.org/10.1073/pnas.83.23.9226

Jacobson, K., Z. Rajfur, E. Vitriol, and K. Hahn. 2008. Chromophore-assisted laser inactivation in cell biology. *Trends Cell Biol.* 18:443–450. http://dx.doi.org/10.1016/j.tcb.2008.07.001

Jahn, R., and D. Fasshauer. 2012. Molecular machines governing exocytosis of synaptic vesicles. *Nature*. 490:201–207. http://dx.doi.org/10.1038/nature11320

Johnson, R.G., and A. Scarpa. 1976. Internal pH of isolated chromaffin vesicles. *J. Biol. Chem.* 251:2189–2191.

Kuijpers, G.A., L.M. Rosario, and R.L. Ornberg. 1989. Role of intracellular pH in secretion from adrenal medulla chromaffin cells. *J. Biol. Chem.* 264:698–705.

Liégeois, S., A. Benedetto, J.M. Garnier, Y. Schwab, and M. Labouesse. 2006. The V0-ATPase mediates apical secretion of exosomes containing Hedgehog-related proteins in *Caenorhabditis elegans*. *J. Cell Biol.* 173:949–961. http://dx.doi.org/10.1083/jcb.200511072

Lindgren, C.A., D.G. Emery, and P.G. Haydon. 1997. Intracellular acidification reversibly reduces endocytosis at the neuromuscular junction. *J. Neurosci.* 17:3074–3084.

Marek, K.W., and G.W. Davis. 2002. Transgenically encoded protein photoinactivation (FlAsH-FALI): acute inactivation of synaptotagmin I. *Neuron*. 36:805–813. http://dx.doi.org/10.1016/S0896-6273(02)01068-1

Martin, B.R., B.N. Giepmans, S.R. Adams, and R.Y. Tsien. 2005. Mammalian cell-based optimization of the biarsenical-binding tetracysteine motif for improved fluorescence and affinity. *Nat. Biotechnol.* 23:1308–1314. http://dx.doi.org/10.1038/nbt1136

Michaelson, D.M., and I. Angel. 1980. Determination of delta pH in cholinergic synaptic vesicles: its effect on storage and release of acetylcholine. *Life Sci.* 27:39–44. http://dx.doi.org/10.1016/0024-3205(80)90017-X

Morel, N. 2003. Neurotransmitter release: the dark side of the vacuolar-H+ATPase. *Biol. Cell*. 95:453–457. http://dx.doi.org/10.1016/S0248-4900(03)00075-3

Morel, N., V. Gérard, and G. Shiff. 1998. Vacuolar H+-ATPase domains are transported separately in axons and assemble in Torpedo nerve endings. *J. Neurochem.* 71:1702–1708. http://dx.doi.org/10.1046/j.1471-4159.1998.71041702.x

Morel, N., Y. Dunant, and M. Israël. 2001. Neurotransmitter release through the V0 sector of V-ATPase. *J. Neurochem.* 79:485–488. http://dx.doi.org/10.1046/j.1471-4159.2001.00611.x

Morel, N., J.C. Dedieu, and J.M. Philippe. 2003. Specific sorting of the a1 isoform of the V-H+ATPase a subunit to nerve terminals where it associates with both synaptic vesicles and the presynaptic plasma membrane. *J. Cell Sci.* 116:4751–4762. http://dx.doi.org/10.1242/jcs.00791

Oot, R.A., and S. Wilkens. 2012. Subunit interactions at the V1-Vo interface in yeast vacuolar ATPase. *J. Biol. Chem.* 287:13396–13406. http://dx.doi.org/10.1074/jbc.M112.343962

Oot, R.A., L.S. Huang, E.A. Berry, and S. Wilkens. 2012. Crystal structure of the yeast vacuolar ATPase heterotrimeric EGC(head) peripheral stalk complex. *Structure*. 20:1881–1892. http://dx.doi.org/10.1016/j.str.2012.08.020

Peri, F., and C. Nüsslein-Volhard. 2008. Live imaging of neuronal degradation by microglia reveals a role for v0-ATPase a1 in phagosomal fusion in vivo. *Cell*. 133:916–927. http://dx.doi.org/10.1016/j.cell.2008.04.037

Peters, C., M.J. Bayer, S. Bühler, J.S. Andersen, M. Mann, and A. Mayer. 2001. Trans-complex formation by proteolipid channels in the terminal phase of membrane fusion. *Nature*. 409:581–588. http://dx.doi.org/10.1038/35054500

Poëa-Guyon, S., M. Amar, P. Fossier, and N. Morel. 2006. Alternative splicing controls neuronal expression of v-ATPase subunit a1 and sorting to nerve terminals. *J. Biol. Chem.* 281:17164–17172. http://dx.doi.org/10.1074/jbc.M600927200

Poëa-Guyon, S., H. Pasquier, F. Mérola, N. Morel, and M. Erard. 2013. The enhanced cyan fluorescent protein: a sensitive pH sensor for fluorescence lifetime imaging. *Anal. Bioanal. Chem.* 405:3983–3987. http://dx.doi.org/10.1007/s00216-013-6860-y

Pollard, H.B., H. Shindo, C.E. Creutz, C.J. Pazoles, and J.S. Cohen. 1979. Internal pH and state of ATP in adrenergic chromaffin granules determined by ^{31}P nuclear magnetic resonance spectroscopy. *J. Biol. Chem.* 254:1170–1177.

Rizo, J., and C. Rosenmund. 2008. Synaptic vesicle fusion. *Nat. Struct. Mol. Biol.* 15:665–674. http://dx.doi.org/10.1038/nsmb.1450

Saw, N.M., S.Y. Kang, L. Parsaud, G.A. Han, T. Jiang, K. Grzegorczyk, M. Surkont, G.H. Sun-Wada, Y. Wada, L. Li, and S. Sugita. 2011. Vacuolar H(+)-ATPase subunits Voa1 and Voa2 cooperatively regulate secretory vesicle acidification, transmitter uptake, and storage. *Mol. Biol. Cell*. 22:3394–3409. http://dx.doi.org/10.1091/mbc.E11-02-0155

Segura, F., M.A. Brioso, J.F. Gómez, J.D. Machado, and R. Borges. 2000. Automatic analysis for amperometrical recordings of exocytosis. *J. Neurosci. Methods*. 103:151–156. http://dx.doi.org/10.1016/S0165-0270(00)00309-5

Shao, E., and M. Forgac. 2004. Involvement of the nonhomologous region of subunit A of the yeast V-ATPase in coupling and in vivo dissociation. *J. Biol. Chem.* 279:48663–48670. http://dx.doi.org/10.1074/jbc.M408278200

Smardon, A.M., and P.M. Kane. 2007. RAVE is essential for the efficient assembly of the C subunit with the vacuolar H(+)-ATPase. *J. Biol. Chem.* 282:26185–26194. http://dx.doi.org/10.1074/jbc.M703627200

Stewart, A.G., and D. Stock. 2012. Priming a molecular motor for disassembly. *Structure*. 20:1799–1800. http://dx.doi.org/10.1016/j.str.2012.10.003

Strasser, B., J. Iwaszkiewicz, O. Michielin, and A. Mayer. 2011. The V-ATPase proteolipid cylinder promotes the lipid-mixing stage of SNARE-dependent fusion of yeast vacuoles. *EMBO J.* 30:4126–4141. http://dx.doi.org/10.1038/emboj.2011.335

Tabares, L., E. Alés, M. Lindau, and G. Alvarez de Toledo. 2001. Exocytosis of catecholamine (CA)-containing and CA-free granules in chromaffin cells. *J. Biol. Chem.* 276:39974–39979. http://dx.doi.org/10.1074/jbc.M106498200

Takamori, S., M. Holt, K. Stenius, E.A. Lemke, M. Grønborg, D. Riedel, H. Urlaub, S. Schenck, B. Brügger, P. Ringler, et al. 2006. Molecular anatomy of a trafficking organelle. *Cell*. 127:831–846. http://dx.doi.org/10.1016/j.cell.2006.10.030

Taupenot, L., K.L. Harper, and D.T. O'Connor. 2005. Role of H+-ATPase-mediated acidification in sorting and release of the regulated secretory protein chromogranin A: evidence for a vesiculogenic function. *J. Biol. Chem.* 280:3885–3897. http://dx.doi.org/10.1074/jbc.M408197200

Thomas, P., J.G. Wong, A.K. Lee, and W. Almers. 1993. A low affinity Ca2+ receptor controls the final steps in peptide secretion from pituitary melanotrophs. *Neuron*. 11:93–104. http://dx.doi.org/10.1016/0896-6273(93)90274-U

Toei, M., R. Saum, and M. Forgac. 2010. Regulation and isoform function of the V-ATPases. *Biochemistry*. 49:4715–4723. http://dx.doi.org/10.1021/bi100397s

Tour, O., R.M. Meijer, D.A. Zacharias, S.R. Adams, and R.Y. Tsien. 2003. Genetically targeted chromophore-assisted light inactivation. *Nat. Biotechnol.* 21:1505–1508. http://dx.doi.org/10.1038/nbt914

Ungermann, C., W. Wickner, and Z. Xu. 1999. Vacuole acidification is required for trans-SNARE pairing, LMA1 release, and homotypic fusion.

Proc. Natl. Acad. Sci. USA. 96:11194–11199. http://dx.doi.org/10.1073/pnas.96.20.11194

Vitale, N., H. Mukai, B. Rouot, D. Thiersé, D. Aunis, and M.F. Bader. 1993. Exocytosis in chromaffin cells. Possible involvement of the heterotrimeric GTP-binding protein G(o). *J. Biol. Chem.* 268:14715–14723.

Vitale, N., A.S. Caumont, S. Chasserot-Golaz, G. Du, S. Wu, V.A. Sciorra, A.J. Morris, M.A. Frohman, and M.F. Bader. 2001. Phospholipase D1: a key factor for the exocytotic machinery in neuroendocrine cells. *EMBO J.* 20:2424–2434. http://dx.doi.org/10.1093/emboj/20.10.2424

Vitale, N., S. Chasserot-Golaz, Y. Bailly, N. Morinaga, M.A. Frohman, and M.F. Bader. 2002. Calcium-regulated exocytosis of dense-core vesicles requires the activation of ADP-ribosylation factor (ARF)6 by ARF nucleotide binding site opener at the plasma membrane. *J. Cell Biol.* 159:79–89. http://dx.doi.org/10.1083/jcb.200203027

Wickner, W., and R. Schekman. 2008. Membrane fusion. *Nat. Struct. Mol. Biol.* 15:658–664. http://dx.doi.org/10.1038/nsmb.1451

Williamson, W.R., D. Wang, A.S. Haberman, and P.R. Hiesinger. 2010. A dual function of V0-ATPase a1 provides an endolysosomal degradation mechanism in *Drosophila melanogaster* photoreceptors. *J. Cell Biol.* 189:885–899. http://dx.doi.org/10.1083/jcb.201003062

Xie, X.S., D. Padron, X. Liao, J. Wang, M.G. Roth, and J.K. De Brabander. 2004. Salicylihalamide A inhibits the V0 sector of the V-ATPase through a mechanism distinct from bafilomycin A1. *J. Biol. Chem.* 279:19755–19763. http://dx.doi.org/10.1074/jbc.M313796200

Yan, P., Y. Xiong, B. Chen, S. Negash, T.C. Squier, and M.U. Mayer. 2006. Fluorophore-assisted light inactivation of calmodulin involves singlet-oxygen mediated cross-linking and methionine oxidation. *Biochemistry*. 45:4736–4748. http://dx.doi.org/10.1021/bi052395a